

Reviewer #1

OVERALL

1) **Comment:** This is a nice work, in which SunDu-derived surface solar radiation (R_s) data are merged with satellite-derived cloud fraction and AOD data to generate high spatial resolution (0.1°) R_s over China. Both direct R_s observations (pyranometer data) at ~100 stations and sun duration records at 2400 stations are used in this study to demonstrate the reliable performances of the merging results. A striking result is that AOD plays a negligible role in the merging results, which indicates that the estimation method of R_s from sunshine measurements is robust and reliable. The result is valuable because long-term AOD retrievals are not accessible when building long-term R_s data. The paper is well organized. I suggest to accept this submission after following issues are addressed.

Reply: The authors would like to thank anonymous referee #1 for his detailed and helpful comments. Below are our point by point responses to his comments.

GENERAL COMMENTS

2) **Comment:** It is not clear how to calculate clear sky R_s although a simple equation is given. A detailed introduction to the method is required since the conclusion mainly relies on the method. I wonder whether aerosol effect on R_s is accounted for by Sunshine duration measurement or by the equation used for the calculation of clear sky R_s . Addition, pls introduce more clearly which data are used in the calculation of clear sky R_s .

Reply: Following anonymous referee #1 comments, we have added the description of the calculation of clear sky R_s (**Lines 255-263**):

“For the clear sky R_s , τ_{c_dir} and τ_{c_dif} are calculated using a modified a broadband radiative transfer model by simplifying Leckner’s spectral model (Leckner, 1978), which the effect of transmittance functions of permanent gas absorption, Rayleigh scattering, water vapour absorption, ozone absorption, and aerosol extinction are parameterized using the surface air temperature, surface pressure, precipitable water, the thickness of the ozone layer, turbidity as inputs (Yang et al., 2006). Calculation of R_s also includes impacts of aerosols because SunDu is impacted by changes in both clouds and aerosols (Wang, 2014).”

Leckner, B. G.: The spectral distribution of solar radiation at the earth's surface—elements of a model, Sol. Energy, 20, 143-150, 1978.

Yang, K., Koike, T., and Ye, B.: Improving estimation of hourly, daily, and monthly solar radiation by importing global data sets, Agric. For. Meteorol., 137, 43-55, 2006.

Wang, K. C., Ma, Q., Li, Z., and Wang, J.: Decadal variability of surface incident solar radiation over China: Observations, satellite retrievals, and reanalyses, Journal of Geophysical Research Atmospheres, 120, 6500-6514, 2015.

3) **Comment:** It was said that site dependent parameters were used in the equation 1 (e.q., a_0 - a_2). I’m not sure how to derive these parameters at each station.

Reply: We added the details of these site dependent parameters (**Lines 249-252**):

“ a_0 , a_1 , and a_2 are the station-dependent parameters by tuning this equation with measurements of R_s and SunDu and then the method is applied regionally (Wang, 2014). Instead using observations from weather stations in Japan (Yang et al., 2006), observations in CMA are used (Wang, 2014).”

Wang, K.C.: Measurement biases explain discrepancies between the observed and simulated decadal variability of surface incident solar radiation, *Scientific Reports*, 4, 6144, 2014.

Yang, K., Koike, T., and Ye, B.: Improving estimation of hourly, daily, and monthly solar radiation by importing global data sets, *Agric. For. Meteorol.*, 137, 43-55, 2006.

4) **Comment:** Frankly speaking, I’m not comfortable with the statement that the CERES EBAF can be taken as the reference. This seems based on the result that the agreement between SunDu-derived R_s and EBAR is much better than that between SunDu-derived R_s and pyranometer measurements. My opinion is that there seems possibility that aerosol effects were not properly accounted for by both SunDu-derived and satellite R_s algorithm. I mean this possibility cannot be fully eliminated, so it is suggestive to discuss this issue in somewhere.

Reply: Thanks for your suggestion, we agree with anonymous referee #1 that the data uncertainties cannot be fully eliminated for both ground observations and satellite retrievals. As mentioned in data section, the uncertainties of CERES EBAF data, reported by (Kato et al., 2018), in all sky global annual mean R_s is 4 W/m². The

descriptions of uncertainties of SunDu derived R_s are added (**Lines 84-87**). The satellite R_s retrievals and SunDu derived R_s are totally independent, but the high agreements of these two datasets indicate that they both are of higher accuracy. We will also discuss this issue in the revised manuscript (**Lines 269-273**):

“Even though, SunDu data do not provide a direct estimate of R_s and have the different sensitivity of atmospheric turbidity changes, compared with R_s observations, they are still a good proxy for variations of R_s (Manara et al., 2017).”

“The satellite R_s retrievals and SunDu derived R_s are totally independent, but the high agreements of these two datasets indicate that they both are of higher accuracy. Similar results are also reported by (Wang et al., 2015) that low agreement between SunDu derived R_s and direct R_s observation is likely due to the directional response errors of the direct observations of R_s .”

Kato, S., Rose, F. G., Rutan, D. A., Thorsen, T. J., Loeb, N. G., Doelling, D. R., Huang, X., Smith, W. L., Su, W., and Ham, S.-H.: Surface Irradiances of Edition 4.0 Clouds and the Earth’s Radiant Energy System (CERES) Energy Balanced and Filled (EBAF) Data Product, *J. Clim.*, 31, 4501-4527, 2018.

Manara, V., Brunetti, M., Maugeri, M., Sanchez-Lorenzo, A., and Wild, M.: Sunshine duration and global radiation trends in Italy (1959–2013): To what extent do they agree?, *journal of geophysical research*, 122, 4312-4331, 2017.

Wang, K.C.: Measurement biases explain discrepancies between the observed and simulated decadal variability of surface incident solar radiation, *Scientific Reports*, 4, 6144, 2014.

MINOR ISSUES

5) **Comment:** Lines 31, ‘Based on the SunDu-derived R_s from 97 meteorological observation stations: : :’, the authors should mention that these 97 stations are co-located with those that direct R_s measurements sites.

Reply: Thanks for your suggestion, we will add this information in **Lines 31-32**:

“Based on the SunDu-derived R_s from 97 meteorological observation stations, which are co-located with those that direct R_s measurement sites...”

6) **Comment:** Lines 130-133, what about the quality of the datasets from (Tang et al. 2019) and (Stengel et al. 2020)? I suggest the authors add detailed descriptions of these datasets.

Reply: we added the description of these dataset (**Lines 136-146**):

“Validation against the BSRN data indicated that SSR-tang have the mean bias error (MBE) of -11.5 W/m^2 and root mean square error (RMSE) of 113.5 W/m^2 for the instantaneous R_s estimates at 10 km scale, but (Tang et al., 2019) point out that care should be taken when using this dataset for trend analysis due to the absent of realistic aerosols input data. Stengel et al. (2020) also show that R_s derived from Cloud_cci AVHRR-PMv3 reveals a very good agreement against BSRN stations, with low standard deviations of 13.8 W/m^2 and correlation coefficients above 0.98. While the bias for shortwave fluxes is small (1.9 W/m^2). However, default an aerosol optical depth

of 0.05 or data from Aerosol cci Level-2 or NASA MODIS Level-2 aerosol data are used in BUGSrad model to calculate clear sky R_s , indicating that impact of aerosols is not perfect parameterized in Cloud_cci AVHRR-PMv3.”

Tang, W., Yang, K., Qin, J., Li, X., and Niu, X.: A 16-year dataset (2000–2015) of high-resolution (3 h, 10 km) global surface solar radiation, Earth Syst. Sci. Data, 11, 1905-1915, 2019.

Stengel, M., Stapelberg, S., Sus, O., Finkensieper, S., Würzler, B., Philipp, D., Hollmann, R., Poulsen, C., Christensen, M., and McGarragh, G.: Cloud_cci Advanced Very High Resolution Radiometer post meridiem (AVHRR-PM) dataset version 3: 35-year climatology of global cloud and radiation properties, Earth Syst. Sci. Data, 12, 41-60, 2020.

7) **Comment:** Lines 164 to 165, the authors show that interpolation results have uncertainties due to the lack of detailed high spatial resolution information. What about the performances of machine learning methods in simulation of R_s . I suggest add more references here.

Reply: we added the description of these dataset (**Lines 183-189**):

“The performances of different machine learning methods have been evaluated in many previous studies, including simulation R_s at regional scale with support of satellite retrievals (Wei et al., 2019; Yeom et al., 2019) and site scale by using routine meteorological observations (Cornejo-Bueno et al., 2019; Hou et al., 2020). Whatever models or training data are selected, the impacts of spatial relationship are not taken

into account in these machine learning methods and therefore large number of input data are required to ensure accuracy.”

Wei, Y., Zhang, X., Hou, N., Zhang, W., Jia, K., and Yao, Y.: Estimation of surface downward shortwave radiation over China from AVHRR data based on four machine learning methods, *Sol. Energy*, 177, 32-46, 2019.

Yeom, J. M., Park, S., Chae, T., Kim, J. Y., and Lee, C. S.: Spatial Assessment of Solar Radiation by Machine Learning and Deep Neural Network Models Using Data Provided by the COMS MI Geostationary Satellite: A Case Study in South Korea, *Sensors (Basel)*, 19, 2019.

Cornejo-Bueno, L., Casanova-Mateo, C., Sanz-Justo, J., and Salcedo-Sanz, S.: Machine learning regressors for solar radiation estimation from satellite data, *Sol. Energy*, 183, 768-775, 2019.

Hou, N., Zhang, X., Zhang, W., Xu, J., Feng, C., Yang, S., Jia, K., Yao, Y., Cheng, J., and Jiang, B.: A New Long-Term Downward Surface Solar Radiation Dataset over China from 1958 to 2015, *Sensors (Basel)*, 20, 2020.

8) **Comment:** Line 178, “0.1” changes to “0.1°”.

Reply: Corrected as suggestions (**Line 199**).

9) **Comment:** Lines 177 to 179, the authors merge the SunDu-derived Rs data with satellite-derived cloud fraction (CF) and AOD data. Why not directly merging the SunDu-derived Rs data with current Rs products?

Reply: Merging current R_s products with SunDu-derived R_s can also be applicable. Since many long-term R_s satellite products use climatology aerosols data as input, in this study, we want to know whether the merged product can achieve reliable R_s data without support of satellite derived aerosols input data.

10) **Comment:** Line 183, "sunDu" changes to "SunDu".

Reply: We have deleted the sentence. (Line 209)

11) **Comment:** Add spatial resolution of each dataset and the references of each dataset in table 2.

Reply: Corrected as suggestions (Line 238).

12) **Comment:** Line 291, why not use MODIS AOD as input data in this study.

Reply: we added the description of why we did not use MODIS AOD as input (Lines 318-322):

"We did not use AOD from MODIS, because MODIS AOD conation missing values and can't meet the requirements of spatiotemporal continuity of AOD input in this study. In addition, MODIS AOD is only available under clear sky conditions while AOD provided by the assimilation system is averaged under all conditions."

13) **Comment:** Lines 316 to 317, SunDu derived R_s also contain the information of clouds, what about merging SunDu-derived R_s data only with AOD data?

Reply: We agree with reviewers that SunDu derived R_s also contain the information of clouds. As cloud data can provide high resolution input data, we use cloud data to improve the spatial resolution of our merged data. We believe that with the support high resolution of AOD data, the merged data can produce more accurate results. However, the spatial resolution of current available AOD are 1 degree.

14) **Comment:** Lines 390 to 392, two validation sites are randomly selected to evaluate the seasonal and annual variations in R_s . I suggest two sites with high AOD values and low AOD values.

Reply: We have checked the selected validation sites. We added this information in the revised manuscript (**Lines 422-423 and Lines 437-438**).

“The multiyear mean of AOD from Changchun and BeiHai are 0.49 and 0.70, respectively.”

15) **Comment:** Line 474, “0.1” changes to “0.1°”.

Reply: Corrected as suggestions (**Line 505**).

16) **Comment:** Line 518, “0.1” changes to “0.1°”.

Reply: Corrected as suggestions (**Line 555**).

17) **Comment:** Lines 535 to 536, deleted “We also plan to expand our R_s dataset from 1983 to 2017 by using AVHRR based cloud retrievals.” Since this study focus the period

from 2000 to 2016.

Reply: Corrected as suggestions.

Reviewer #2

OVERALL

1) **Comment:** This study attempts to generate a high resolution surface solar radiation (R_s) dataset. The idea is to construct a linear model between station based R_s , cloud fraction and AOD, and applies the model to the full study domain (China). While this dataset can be potentially useful, I don't understand how this approach could achieve a better accuracy than CERES 1 degree R_s product. This is because: (1) although the SunDu R_s can represent a much smaller area than the CERES 1 degree grid, SunDu R_s is validated using CERES R_s , which means that SunDu R_s cannot have a higher accuracy than CERES R_s , even at the 1 degree scale; (2) the AOD data used is still at 1 degree resolution. This does not add much finer information and may be the reason why AOD has little impact on the prediction results. Overall, I don't see much value in this study unless the above question is addressed. Please see the specific comments below:

Reply: We realize that we have not clearly explained the significance of our work to generate high spatial resolution R_s data and the comparison results. We carefully think about all comments from anonymous referee #2. Below are our point by point responses to the comments.

MAJOR COMMENTS

2) **Comment:** The authors used SunDu R_s to train the model and to generate the high resolution R_s dataset. However, SunDu R_s is validated against CERES R_s , assuming that the latter has higher accuracy. On one hand, using grid based data to validate station

based data is not appropriate. There can be a lot of variability within this 1 degree box. The authors did compare SunDu R_s with observed R_s but argued that their agreement is not as good as that between SunDu R_s and CERES R_s , and that the agreement between the latter two proves the reliability of SunDu R_s . I don't agree with this argument. SunDu R_s should be directly validated against surface observed R_s . On the other hand, if CERES R_s is better than SunDu R_s , what's the point of using SunDu R_s to generate the 0.1 degree dataset? I guess using CERES R_s with 0.1 cloud and AOD would achieve at least the same accuracy, if not better. Yet, it has the advantage of full spatial coverage than SunDu R_s .

Reply: We realize that we have not clearly explained the significance of our work and comparison results. In this study, we aim to build a reliable high resolution grid R_s data by establishing the physical spatial relationship between ground based SunDu derived R_s data with high resolution cloud satellite data with AOD to avoid the disadvantage of CERES for capturing the variability of R_s within a 1 degree box. We have refined the description of our goals in the end of introduction (**Lines 205-209**): "Since current R_s high quality R_s such as CERES EBAF have low spatial resolution, the output of this study provides a reliable high resolution grid R_s data to avoid the disadvantage of CERES EBAF for capturing the variability of R_s within a 1 degree box and provide guidance to merge multisource data to generate long-term R_s data over China." We know that direct comparison between grid based data and station based data is not perfect. "However we show that the satellite R_s retrievals and SunDu derived R_s are totally independent, but the high agreements of these two datasets indicate that they

both are of higher accuracy. Similar results are also reported by (Wang et al., 2015) that low agreement between SunDu derived R_s and direct R_s observation is likely due to the directional response errors of the direct observations of R_s ” (Lines 270-273). We know that direct comparison between grid based data and station based data is not perfect. But direct comparison are widely used as a tradeoff way for validation in many studies due to lack of reliable high resolution grid R_s data. In this study, we aim to build this reliable high resolution grid R_s data. One may argue that using CERES R_s with 0.1 cloud and AOD can also produce high resolution R_s data. However, there are large amount of input data are require to ensure the accuracy of CERES. Most of these input data in CERES have low spatial resolution and limited spatial coverage and are only available after 2000. SunDu R_s have long time records with large spatial coverage. The merged SunDu derived R_s data can overcome these disadvantages of CERES and have the possibilities to build long term R_s by using AVHRR data.

3) **Comment:** To proof the effect of fine resolution processing, a direct comparison with CERES should be provided. The authors can interpolate the CERES R_s to 0.1 degree and compare with their results. How difference are they? Are the differences physically explainable (i.e., related to cloud variability?).

Reply: Thanks for your suggestion. We have discussed this issue in the discussion section (Lines 542-545)

“By using spatial interpolation method, CERES R_s can also be downscaled to 1km or 30m. These interpolated CERES R_s data cannot represent the detailed R_s distributions at spatial resolution of 1km or 30m. Without additional high spatial resolution data,

interpolated cannot capture more detail variability of R_s . High spatial resolution cloud data can provide more detail information of cloud variability.”

MINOR COMMENTS

4) **Comment:** What is the reason of the lower agreement between SunDu R_s and observed R_s ?

Reply: The reason of the lower agreement between SunDu R_s and observed R_s have added in the revised manuscript (**Lines 271-273**)

“Similar results are also reported by (Wang et al., 2015) that low agreement between SunDu derived R_s and direct R_s observation is likely due to the directional response errors of the direct observations of R_s .”

Wang, K. C., Ma, Q., Li, Z., and Wang, J.: Decadal variability of surface incident solar radiation over China: Observations, satellite retrievals, and reanalyses, *Journal of Geophysical Research Atmospheres*, 120, 6500-6514, 2015.

5) **Comment:** Why using CERES 1degree AOD? If spatial resolution matters, there are much finer products, such as the MODIS 1km and MODIS 3km products.

Reply: We have added the reasons in (**Lines 319-323**):

“We did not use AOD from MODIS, because MODIS AOD conation missing values and can't meet the requirements of spatiotemporal continuity of AOD input in this study. In addition, MODIS AOD is only available under clear sky conditions while AOD provided by the assimilation system is averaged under all conditions.”

6) **Comment:** There are remote locations with very few SunDu stations, such as the

Tibet plateau, are the relationships applicable?

Reply: As shown in figure 9, the regional mean of the annual anomaly of the surface solar radiation (R_s) for zone II and zone VIII which are the regions such as the Tibet plateau. We notice that the merged R_s (GWR-CF-AOD) can produce consistent variation of R_s compared with observed data, indicating the relationships are applicable.

7) **Comment:** It would be interesting to look at the spatial distribution of the coefficients. This can tell us some information about where clouds make a bigger impact and where aerosols are important.

Reply: According to the figure 6 in our previous study (Feng and Wang, 2019), cloud fraction shows strong negative correlation with R_s in most parts of China, while slight weak correlation coefficient near the north border of China. While clear sky R_s , which are primarily impact by the atmospheric aerosol loading, generally have small the correlation coefficient with R_s in most parts China.

Feng, F. and Wang, K.: Determining Factors of Monthly to Decadal Variability in Surface Solar Radiation in China: Evidences from Current Reanalyses, J. Geophys. Res. Atmos., 124, 9161-9182, 2019.

8) **Comment:** What's the unit of Figure 2?

Reply: We have added this information in the revised paper (**Lines 286-287**):

“The unit of y-axis are W/m^2 ”

Merging ground-based sunshine duration observations with satellite cloud and aerosol retrievals to produce high resolution long-term surface solar radiation over China

Fei Feng¹ † and Kaicun Wang² †

1. College of Forestry, Beijing Forestry University, Beijing 100083, China

2. State Key Laboratory of Earth Surface Processes and Resource Ecology, College of Global Change and Earth System Science, Beijing Normal University, Beijing, 100875, China

†These authors contributed equally to this work

Corresponding Author:

Fei Feng, College of Forestry, Beijing Forestry University, Email: forgetbear@bjfu.edu.cn;

Kaicun Wang, College of Global Change and Earth System Science, Beijing Normal University. Email: kcwang@bnu.edu.cn; Tel: +086 10-58803143; Fax: +086 10-58800059.

Abstract

Although great progress has been made in estimating surface solar radiation (R_s) from meteorological observations, satellite retrieval and reanalysis, getting best estimated long-term variations in R_s are sorely needed for climate studies. It has been shown that sunshine duration (SunDu)-derived R_s data can provide reliable long-term variability, but are available at sparsely distributed weather stations. Here, we merge SunDu-derived R_s with satellite-derived cloud fraction and aerosol optical depth (AOD) to generate high spatial resolution (0.1°) R_s over China from 2000 to 2017. The geographically weighted regression (GWR) and ordinary least squares regression (OLS) merging methods are compared, and GWR is found to perform better. Based on the SunDu-derived R_s from 97 meteorological observation stations, which are co-located with those that direct R_s measurement sites, the GWR incorporated with satellite cloud fraction and AOD data produces monthly R_s with $R^2 = 0.97$ and standard deviation = 11.14 W/m^2 , while GWR driven by only cloud fraction produces similar results with $R^2 = 0.97$ and standard deviation = 11.41 W/m^2 . This similarity is because SunDu-derived R_s has included the impact of aerosols. This finding can help to build long-term R_s variations based on cloud data, such as Advanced Very High Resolution Radiometer (AVHRR) cloud retrievals, especially before 2000, when satellite AOD retrievals are not unavailable. The merged R_s product at a spatial resolution of 0.1° in this study can be downloaded at <https://doi.pangaea.de/10.1594/PANGAEA.921847> (Feng and Wang, 2020).

Introduction

A clear knowledge of variations in surface solar radiation (R_s) is vitally important for an improved understanding of the global climate system and its interaction with human activity (Jia et al., 2013; Myers, 2005; Schwarz et al., 2020; Wang and Dickinson, 2013; Wild, 2009, 2017; Zell et al., 2015). [Direct measurements](#) have shown that R_s has significant decadal variability, namely, a decrease (global dimming) from the 1950s to the late 1980s and subsequent increase (global brightening) (Wild, 2009). The variation in R_s is closely related to [the Earth's water cycle](#), the whole biosphere, and the amount of available solar energy. This situation emphasizes the urgency to develop reliable R_s products to obtain the variability in R_s .

Great progress has been made in the detection of variability in R_s by meteorological observations, satellite retrieval and radiation transfer model simulations or reanalysis R_s products in previous studies (Rahman and Zhang, 2019; Wang et al., 2015). However, each estimation has its advantages and disadvantages. Direct observed data provide accurate R_s records [at short time scales](#); however, careful calibration and instrument maintenance are needed [to maintain its long-term homogeneity](#). Previous studies have reported that direct observed R_s [over China](#) may have major inhomogeneity problems due to sensitivity drift and instrument replacement (Wang, 2014; Wang et al., 2015; Yang et al., 2018). Before 1990, the imitations of the USSR pyranometers had different degradation rates of the thermopile, resulting in an important sensitivity drift. To overcome radiometer ageing [problem](#), China replaced its instruments from 1990 to 1993. However, the new solar trackers failed frequently and introduced a [high data missing rate](#) for the direct radiation component of R_s (Lu and Bian, 2012; Mo et al., 2008). After 1993, although the instruments were substantially improved, the Chinese-developed pyranometers still had high thermal offset with directional response errors,

and the stability of these instruments was also worse than that of the World Meteorological Organization (WMO) recommended first-class pyranometers (Lu et al., 2002; Lu and Bian, 2012; Yang et al., 2010). Yang et al. (2018) show that nearly half of observed R_s (60 out of the 119 R_s observed stations) have inhomogeneity issues. These artificial changes points in observed R_s are mainly caused by instrument change (42 shifts), stations relocation (34 shifts), observation schedule change (20 shifts) and remaining 64 changepoints could not be identified.

SunDu data are relatively widely distributed and have a long-term record (Sanchezlorenzo et al., 2009; Wild, 2009). Existing studies have also confirmed that SunDu-derived R_s data are reliable R_s data, which can capture long-term trends of R_s and reflect the impacts of both aerosols and clouds at time scales ranging from daily to decadal (Feng and Wang, 2019; Manara et al., 2015; Sanchezlorenzo et al., 2013; Sanchezromero et al., 2014; Tang et al., 2011; Wang et al., 2012b; Wild, 2016). Even though, SunDu data do not provide a direct estimate of R_s and have the different sensitivity of atmospheric turbidity changes, compared with R_s observations, they are still a good proxy for variations of R_s (Manara et al., 2017).

Sunshine duration observations collected at weather stations in China have been used to reconstruct long-term R_s (Che et al., 2005; Feng et al., 2019; He et al., 2018; He and Wang, 2020; Jin et al., 2005; Shi et al., 2008; Yang et al., 2006; Yang et al., 2020). Based on the global SunDu-derived R_s records, He et al. (2018) found that SunDu permitted a revisit of global dimming from the 1950s to the 1980s over China, Europe, and the USA, with brightening from 1980 to 2009 in Europe and a declining trend R_s from 1994 to 2010 in China. (Wang et al., 2015) found that the dimming trend from 1961 to 1990 and nearly constant zero trend after 1990 over China, as calculated from the SunDu-derived R_s , was consistent with independent estimates of AOD (Luo et al.,

2001); they also observed changes in the diurnal temperature range (Wang et al., 2012a; Wang and Dickinson, 2013) and the observed pan evaporation (Yang et al., 2015). Although direct observations and SunDu-derived R_s can provide accurate long-term variations in R_s , both direct observations and sunshine duration records are often sparsely spatially distributed.

Satellite R_s retrievals and radiation transfer model simulations or reanalysis R_s products can provide R_s estimation with global coverage at high spatial resolution. However, model simulations and reanalysis R_s products have substantial biases due to the deficiency of simulating cloud and aerosol quantities (Feng and Wang, 2019; Zhao et al., 2013). Previous comparative studies have shown that the accuracies of R_s from reanalyses are lower than those of satellite products (Wang et al., 2015; Zhang et al., 2016) due to the good capability of capturing the spatial distribution and dynamic evolution of clouds in satellite remote sensing data.

Table 1 lists the current satellite-based R_s products, which have been widely validated in previous studies. Zhang et al. (2004) found that the monthly International Satellite Cloud Climatology Project-Flux Data (ISCCP-FD) R_s product had a positive bias of 8.8 w/m² using Global Energy Balance Archive (GEBA) archived data as a reference. By comparing 1151 global sites, Zhang et al. (2015) evaluated four satellite-based R_s products, including ISCCP-FD, the Global Energy and Water Cycle Experiment-Surface Radiation Budget (GEWEX-SRB), the University of Maryland/Shortwave Radiation Budget (UMD-SRB) and the Earth's Radiant Energy System energy balanced and filled product (CERES EBAF), and concluded that CERES EBAF shows better agreement with observations than other products. A similar overall good performance of CERES EBAF can also be found (Feng and Wang, 2018; Ma et al., 2015).

Table 1. Current satellite-derived surface solar radiation (R_s) products

Satellite R_s product	Source	Spatial resolution	Time range
ISCCP-FD	ISCCP	2.5°	1983-2009
GEWEX-SRB	ISCCP-DX	1°	1983-2007
UMD-SRB	METEOSAT-5	0.5°	1983-2007
GLASS-DSR	Terra/Aqua, GOES, MSG, MTSAT	0.05°	2008-2010
CLARA-A2	AVHRR	0.25°	1982-2015
MCD18A1	Terra/Aqua, MODIS	5.6 km	2001-present
Himawari-8 SWSR	Himawari-8	5 km	2015-present
SSR-tang	ISCCP-HXG, ERA5, MODIS	10 km	1982-2017
Cloud_cci AVHRR-PMv3	AVHRR/CC4CL	0.05°	1982-2016

Although CERES EBAF uses more accurate input data to provide R_s data, its spatial resolution is only 1° (Kato et al., 2018). Since 2010, new-generation geostationary satellites have provided opportunities for high temporal and spatial resolution R_s data, such as Himawari-8 (Hongrong et al., 2018; Letu et al., 2020). However, the time span of the new-generation satellite-based R_s product is short. The long-term AVHRR records provide the possibility of building long-term radiation datasets. The CCloud, Albedo and RAdiation dataset, the AVHRR-based data-second edition (CLARA-A2), covers a long time period, but the spatial resolution is only 0.25° (Karlsson et al., 2017). Recently, Tang et al. (2019) built a satellite-based R_s (SSR-tang) dataset using ISCCP-HXG cloud data. By using a variety of cloud properties derived from AVHRR, Stengel et al. (2020) presented the Cloud_cci AVHRR-PMv3 dataset generated within the Cloud_cci project.

Validation against the BSRN data indicated that SSR-tang have the mean bias error (MBE) of -11.5 W/m² and root mean square error (RMSE) of 113.5 W/m² for the instantaneous R_s estimates at 10 km scale, but Tang et al. (2019) point out that care should be taken when using this dataset for trend analysis due to the absent of realistic aerosols input data. Stengel et al. (2020) also show that R_s derived from Cloud_cci

AVHRR-PMv3 reveals a very good agreement against BSRN stations, with low standard deviations of 13.8 W/m^2 and correlation coefficients above 0.98. While the bias for shortwave fluxes is small (1.9 W/m^2). However, default an aerosol optical depth of 0.05 or data from Aerosol cci Level-2 or NASA MODIS Level-2 aerosol data are used in BUGSrad model to calculate clear sky R_s , indicating that impact of aerosols is not perfect parameterized in Cloud_cci AVHRR-PMv3.

On the other hand, the long-term cloud records also contain uncertainties. For example, ISCCP cloud products, which directly combine geostationary and polar orbiter satellite-based cloud data, have large inhomogeneity due to different amounts of data from polar orbit and geostationary satellites and their different capabilities for detecting low-level clouds (Dai et al., 2006; Evan et al., 2007). This inhomogeneity of the cloud products might introduce significant inhomogeneity to the R_s values calculated from the cloud products (Montero-Martín et al., 2020; Pfeifroth et al., 2018b), and R_s long-term variability estimation still needs improvement.

Efforts have been made to further improve R_s products. Merging multisource data has become an effective empirical method for improving the quality of R_s products (Camargo and Dorner, 2016; Feng and Wang, 2018; Hakuba et al., 2014; Journée et al., 2012; Lorenzo et al., 2017; Ruiz-Arias et al., 2015). For instance, to produce spatiotemporally consistent R_s data, multisource satellite data are used in Global LAnd Surface Satellite (GLASS) R_s products (Jin et al., 2013). By merging reanalysis and satellite R_s data by the probability density function-based method, the reanalysis R_s biases can be substantially reduced (Feng and Wang, 2018). This finding suggests that fusion methods are effective ways to improve the estimation of R_s , especially when R_s impact factors are considered (Feng and Wang, 2019). Although linear regression fusion methods can produce R_s data incorporated with R_s impact factors, the stable regression

parameters might have negative effects on the final fusion results due to the complex characteristics of R_s spatial-temporal variability.

On the other hand, the spatial resolution of R_s data is crucial for regional meteorology studies, as the minimum requirement of the spatial resolution of R_s data, as suggested by the Observing Systems Capabilities Analysis and Review of WMO OSCAR), is 20 km (Huang et al., 2019). Interpolation methods are often included in R_s fusion methods to further improve the spatial resolutions of R_s data (Loghmari et al., 2018). For example, Zou et al. (2016) estimated global solar radiation using an artificial neural network based on an interpolation technique in southeast China. By integrating R_s data from 13 ground stations with Meteosat Second Generation satellite R_s products, Journée and Bertrand (2010) found that kriging with the external drift interpolation method performed better than mean bias correction, interpolated bias correction and ordinary kriging with satellite-based correction. However, interpolation results have uncertainties due to the lack of detailed high spatial resolution information. Although traditional linear regression fusion methods can incorporate high spatial resolution data during the fusion process, the impacts of the stable regression parameters need further investigation.

The performances of different machine learning methods have been evaluated in many previous studies, including simulation R_s at regional scale with support of satellite retrievals (Wei et al., 2019; Yeom et al., 2019) and site scale by using routine meteorological observations (Cornejo-Bueno et al., 2019; Hou et al., 2020). Whatever models or training data are selected, the impacts of spatial relationship are not taken into account in these machine learning based model and therefore large number of input data are required to ensure accuracy.

Geographically weighted regression (GWR) is an extension of the traditional

regression model by allowing the relationships between dependent and explanatory variables to vary spatially. Researchers have examined and compared the applicability of GWR for the analysis of spatial data relative to that of other regression methods (Ali et al., 2007; Gao et al., 2006; Georganos et al., 2017; LeSage, 2004; Sheehan et al., 2012; Zhou et al., 2019a). Due to the large spatial heterogeneity of R_s over China, the GWR method might produce accurate R_s variability estimations with an improved spatial resolution.

This study is established to merge SunDu-derived R_s data with satellite-derived cloud fraction (CF) and AOD data to generate high spatial resolution (0.1°) R_s over China from 2000 to 2017. The GWR and ordinary least squares (OLS) regression merging methods are compared. CF and AOD are important R_s impact factors, however, many long-term R_s satellite products use climatology aerosols data as input. Whether much improvement is made in merging SunDu-derived R_s by incorporating AOD is also evaluated in this study, instead of evaluating direct merging current R_s products with SunDu-derived R_s . Since current R_s high quality R_s such as CERES EBAF have low spatial resolution, the output of this study provides a reliable high resolution grid R_s data to avoid the disadvantage of CERES EBAF for capturing the variability of R_s within a 1 degree box and provide guidance to merge multisource data to generate long-term R_s data over China.

1. Data and Methodology

2.1. Ground-based observations

2.2.1 Direct observations

R_s direct observations from 2000 to 2017 are obtained from the China Meteorological Data Service Center (CMDC, <http://data/cma/cn/>) of the China Meteorological Administration (CMA). TBQ-2 pyranometers and DFY4 pyranometers

have been used to measure R_s since 1993. Daily R_s values from 97 R_s stations are collected, and we calculated monthly R_s values by averaging daily R_s values when daily observed data are available for more than 15 days for each month at each radiation station. These monthly R_s values from direct measurements and collocated SunDu-derived R_s are used as independent reference data to investigate the performances of the fusion methods (**Fig. 1**). The whole area over China is further divided into nine zones by the K-mean cluster method based on geographic locations and multiyear mean R_s using 97 R_s direct observation sites, as shown in **Figure 1**. The download instructions of the R_s direct observations can be found in **table 2**.

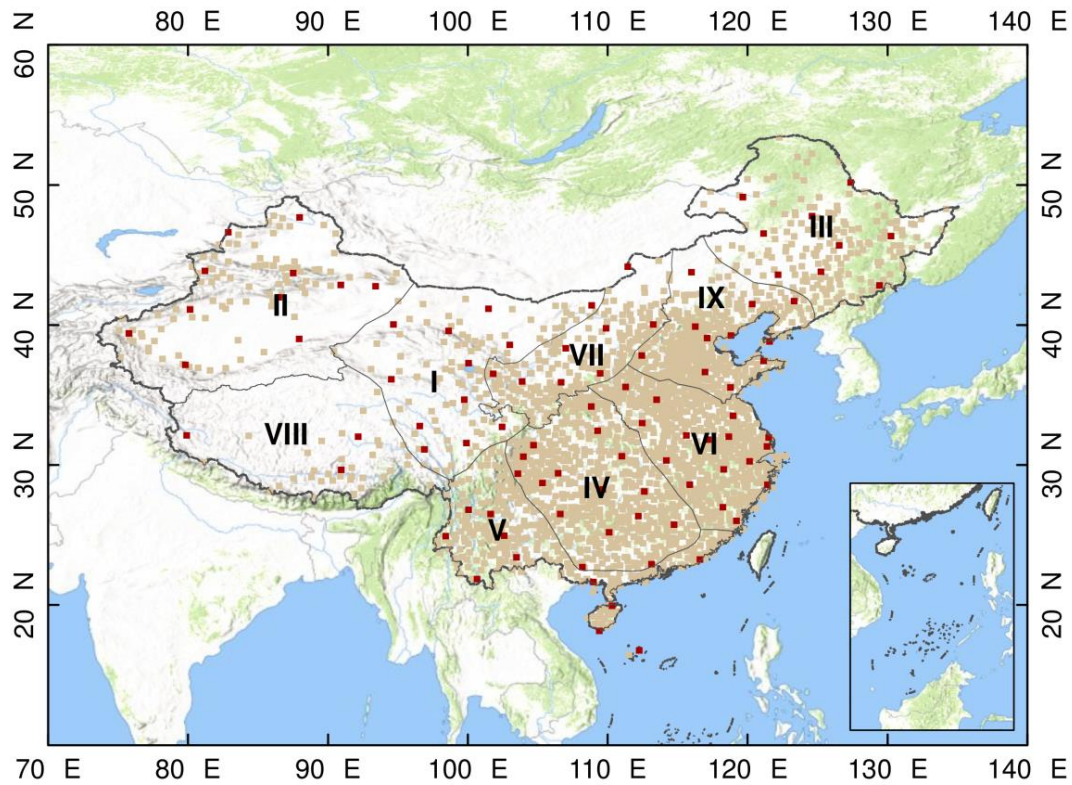


Figure 1. The 2,400 sunshine duration (SunDu) merging sites are shown as light brown points, and 97 independent validation sites, including R_s direct measurements and SunDu-derived R_s measurements, are shown as brown red points. The whole region is classified into nine subregions (I to IX) by the K-mean cluster method based on geographic locations and multiyear mean R_s using 97 R_s direct observation sites. The

base hillshade map was produced by an elevation map of China using the global digital elevation model (DEM) derived from the Shuttle Radar Topography Mission 30 (SRTM30) dataset.

Table 2. Summary of availability information for all source data used in this study. CMDC is the China Meteorological Data Service Center. SunDu is the sunshine duration data. R_s is surface solar radiation and AOD is the aerosols optical depth.

Data Source	Derived Parameters	Spatial resolution	Version	Access Point	Notes	Reference
Direct R_s measurement data from CMDC	R_s	-	Version 1.0	http://data/cma/cn/	Authentication is required for the China data use policy	-
SunDu observations and other meteorological data	R_s	-	Version 1.0	http://data/cma/cn/	Authentication is required for the China data use policy	-
CERES EBAF	R_s	1 degree	Ed4.1	https://ceres.larc.nasa.gov/data/#ebaf-level-3b	A email address to order the data	(Kato et al., 2018)
CERES SYN1deg	AOD	1 degree	Ed4A	https://ceres.larc.nasa.gov/data/#syn1deg-level-3	A email address to order the data	(Rutan et al., 2015)
MODAL2 M CLD	cloud fraction	0.1 degree	-	https://neo.sci.gsfc.nasa.gov/view.php?datasetId=MODAL2_M_CLD_FR	Directly download	(Platnick et al., 2017)

2.2.2 SunDu-derived R_s

Sunshine duration observations (SunDu) and other meteorological data (e.g., air temperature, relative humidity and surface pressure) from 1980 to 2017, which were

collected from approximately 2,400 meteorological stations (<http://data/cma/cn/>) from the CMA, are used to calculate the SunDu-derived R_s (**Fig. 1**). R_s values are calculated following the method of the revised Ångström-Prescott equation (Eq. (1-2)) (He et al., 2018; Wang, 2014; Wang et al., 2015; Yang et al., 2006).

$$\frac{R_s}{R_c} = a_0 + a_1 \frac{n}{K} + a_2 \left(\frac{n}{K}\right)^2 \quad (1)$$

$$R_c = \int (\tau_{c_dir} + \tau_{c_dif}) \times I_0 dt \quad (2)$$

where n represents the measured SunDu, and K represents the theoretical value of the SunDu. a_0 , a_1 , and a_2 are the station-dependent parameters by tuning this equation with measurements of R_s and SunDu and then the method is applied regionally (Wang, 2014). Instead using observations from weather stations in Japan (Yang et al., 2006), observations in CMA are used (Wang, 2014). R_c is the daily total solar radiation at the surface under clear-sky conditions (Eq. 2). τ_{c_dir} and τ_{c_dif} represent the direct radiation transmittance and the diffuse radiation transmittance under clear-sky conditions. I_0 is the solar irradiance at the top of the atmosphere (TOA). For the clear sky R_s , τ_{c_dir} and τ_{c_dif} are calculated using a modified a broadband radiative transfer model by simplifying Leckner's spectral model (Leckner, 1978), which the effect of transmittance functions of permanent gas absorption, Rayleigh scattering, water vapour absorption, ozone absorption, and aerosol extinction are parameterized using the surface air temperature, surface pressure, precipitable water, the thickness of the ozone layer, turbidity, sunshine duration as inputs (Yang et al., 2006). Calculation of R_s also includes impacts of aerosols because SunDu is impacted by changes in both clouds and aerosols (Wang, 2014).

Based on the classified subregions using 97 direct R_s observations in **Figure 1**, the intercomparison results in **Figure 2** and **Figure 3** show that the agreement between SunDu-derived R_s and CERES EBAF R_s estimates is better than that between the direct

observations and SunDu-derived R_s estimates, which is likely due to the inhomogeneity issue of direct R_s observations over China, as mentioned in many previous studies (Wang, 2014; Yang et al., 2018). The satellite R_s retrievals and SunDu derived R_s are totally independent, but the high agreements of these two datasets indicate that they both are of higher accuracy. Similar results are also reported by (Wang et al., 2015) that low agreement between SunDu derived R_s and direct R_s observation is likely due to the directional response errors of the direct observations of R_s .

The SunDu-derived R_s observations, excluding SunDu observations located at direct observation sites, are used for merging. Ten percent merging observations are randomly selected for GWR parameter optimization. The download instructions of the SunDu observations can be found in **table 2**.

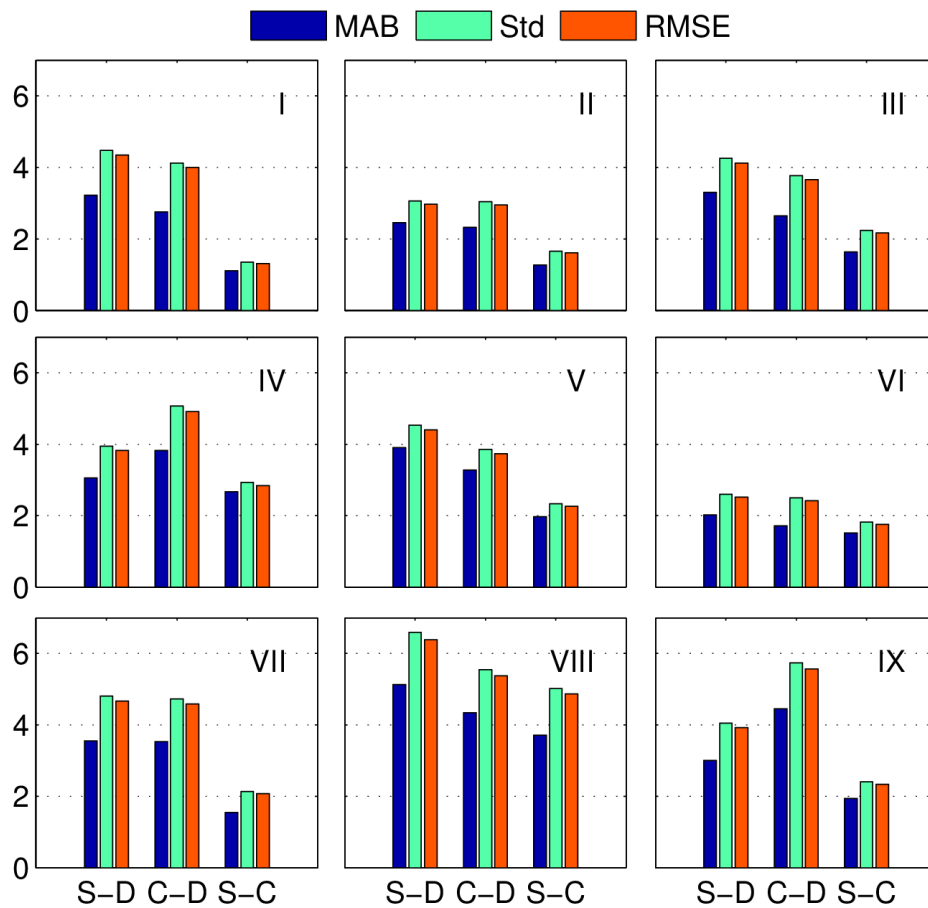


Figure 2. Statistical summary of annual anomaly R_s from direct observed R_s , SunDu-derived R_s and CERES EBAF R_s estimates in different subregions. The statistics include the mean absolute bias (MAB), standard deviation (Std) and root mean square error (RMSE). We use MAB due to the cancelling out effect of positive bias and negative bias. Nine subregions (I to IX) over China are shown in Figure 1. S-D represent comparisons between SunDu-derived R_s and directly observed R_s . C-D represent comparison between CERES EBAF R_s and directly observed R_s . S-C represent comparisons between SunDu-derived R_s and CERES EBAF R_s . The unit of y-axis are w/m^2 .

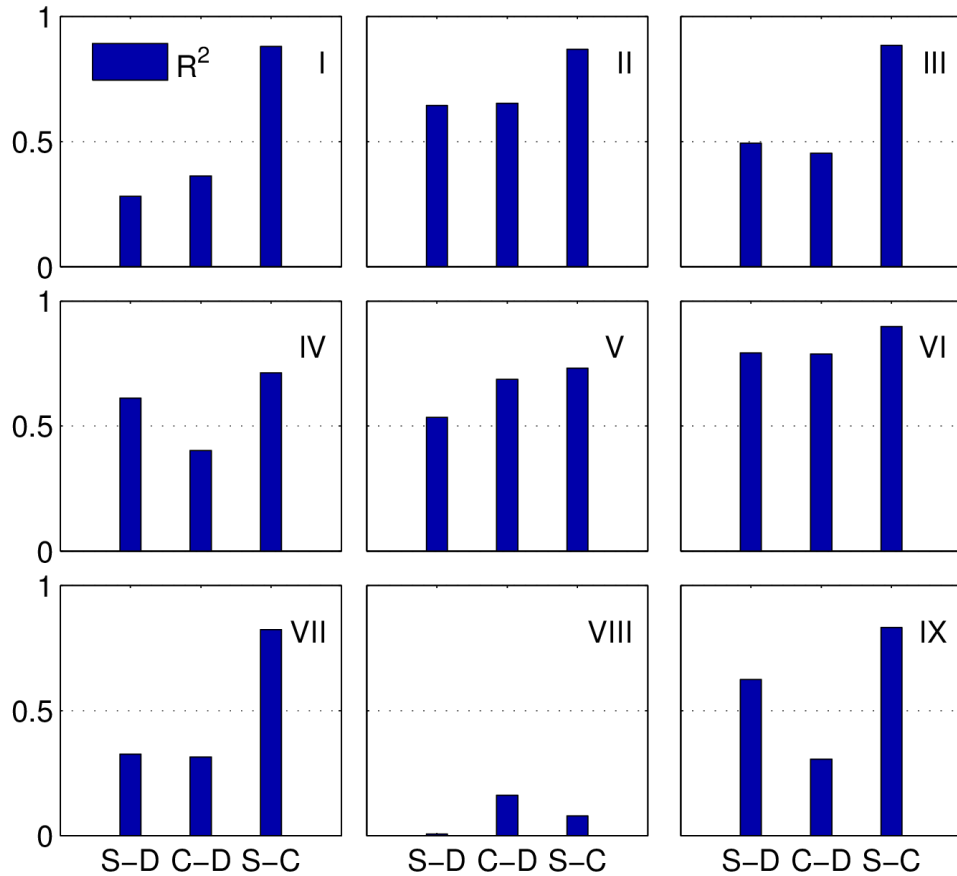


Figure 3. Similar to Figure 2, but this statistical summary is for R^2 .

2.2. Satellite data

R_s data from the Clouds and Earth's Radiant Energy System energy balanced and

filled product (CERES Synoptic (CERES) EBAF) surface product (edition 4.1) (Kato et al., 2018), cloud fraction from MODAL2 M CLD data product (Platnick et al., 2017) and AOD from the CERES SYN1deg) edition 4A product (Doelling et al., 2013) are collected in this study. CERES EBAF R_s data are used as reference data. AOD from CERES SYN1deg and cloud fraction from MODAL2 M CLD are used as input data for fusion methods.

CERES is a 3-channel radiometer measuring three filtered radiances, including shortwave (0.3-5 μm), total (0.3-200 μm) and window (8-12 μm). R_s from CERES EBAF are adjusted using radiative kernels, including bias correction and Lagrange multiplier processes. The input data of CERES EBAF are adjusted during the product generating process constrained by CERES observations at the TOA. The biases in temperature and specific humidity from the Goddard Earth Observing System (GEOS) reanalysis are adjusted by atmospheric infrared sounder (AIRS) data. Cloud properties, such as optical thickness and emissivity, from MODIS and geostationary satellites are constrained by cloud profiling radar, Cloud-Aerosol Lidar, and Infrared Pathfinder Satellite Observations (CALIPSO) detectors and CloudSat. The uncertainties of CERES EBAF data, reported by (Kato et al., 2018), in all sky global annual mean R_s is 4 W m^{-2} . Previous studies (Feng and Wang, 2019; Feng and Wang, 2018; Ma et al., 2015; Wang et al., 2015) have shown that the CERES EBAF surface product provides reliable estimations of R_s .

CERES SYN1deg AOD derived from an aerosol transport model, named Atmospheric Transport and Chemistry Modelling (MATCH) (Collins et al., 2001), which assimilates MODIS AOD data, is used to obtain spatiotemporally consistent AOD data. Different aerosol constituents, including small dust ($<0.5 \mu\text{m}$), large dust ($>0.5 \mu\text{m}$), stratosphere, sea salt, soot and soluble, are used to compute the optical

thickness for a given constituent optical thickness for a given constituent. We did not use AOD from MODIS, because MODIS AOD conation missing values and can't meet the requirements of spatiotemporal continuity of AOD input in this study. In addition, MODIS AOD is only available under clear sky conditions while AOD provided by the assimilation system is averaged under all conditions.

Cloud fraction data from MODAL2 M CLD are collected as input cloud fraction data with a spatial resolution of 0.1° and time span from 2000 to 2017 (Platnick et al., 2017). The MODAL2 M CLD data are synthesized based on the cloud data from MOD06. Cloud fraction data from MOD06 are generated by the cloud mask product of MOD35 with a spatial resolution of 1 km. The MOD35 cloud mask is determined by applying appropriate single field of view (FOV) spectral tests to each pixel with a series of visible and infrared threshold and consistency tests. Each land type has different algorithms and thresholds for the tests. For each pixel test, an individual confidence flag is determined and then combined to produce the final cloud mask flag. The three confidence levels included in the cloud mask flag output are (i) high confidence for cloudless pixels (Group confidence values > 0.95); (ii) low confidence for unobstructed views on the surface (Group confidence values $Q \leq 0.66$); and (iii) values between 0.66 and 0.95, and spatial and temporal continuity tests are further applied to determine whether the pixel is absolutely cloudless. Then, the cloud fraction is calculated from the 5×5 -km cloud mask pixel groupings, i.e., given the 25 pixels in the group, the cloud fraction for the group equals the number of cloudy pixels divided by 25.

2.3. Methods

2.3.1 Fusion models

OLS regression and GWR are used to build fusion methods for estimating R_s data. Clouds fraction and AOD have been important factors that affect variations in R_s . We compare different combinations of input data for the fusion methods, which can be

classified into two types. The first type only contains cloud fraction data. The second type contains clouds fraction and AOD (Feng and Wang, 2020).

The OLS regression model is a commonly used model to estimate dependent variables by minimizing the sum of square differences between the independent and dependent variables. GWR is a regression model that allows the relationships between the independent and dependent variables to vary by locality (Brunsdon et al., 2010; Brunsdon et al., 1998). GWR deviates from the assumption of homoskedasticity or static variance but calculates a specific variance for data within a zone or search radius of each predictor variable (Brunsdon et al., 1998; Fotheringham et al., 1996; Sheehan et al., 2012). The regression coefficients in GWR are not based on global information; rather, they vary with location, which is generated by a local regression estimation using subsampled data from the nearest neighbouring observations. The principle of GWR is described as follows:

$$y_i = \delta(i) + \sum_k \delta_k(i)x_{ik} + \varepsilon_i \quad (3)$$

where y_i is the value of R_s unit i ; $i=1,2,\dots,n$, n denotes location i , x_{ik} indicates the value of the x_{ik} variable, such as cloud fraction and AOD, and ε denotes the residuals. $\delta(i)$ is the regression intercept. $\delta_{k(i)}$ is the vector of regression coefficients determined by spatial weighting function $w(i)$, which is the weighting function quantifying the proximities of location i to its neighbouring observation sites; X is the variable matrix, and b is the bias vector.

$$\delta_k(i) = (X^T w(i)X)^{-1} X^T w(i)b \quad (4)$$

The weighting functions are generally determined using the threshold method, inverse distance method, Gauss function method, and Bi-square method. Due to the irregular distribution of observation sites and computer ability, the adaptive Gaussian

function method is selected as a weighting function that varies in extent as a function of R_s observation site density.

$$w_{ij} = \exp(-(d_{ij}/b)^2) \quad (5)$$

where w_{ij} is the weighting function for observation site j that refers to location i ; d_{ij} denotes the Euclidian distance between j and i ; and b is the size of the neighbourhood, the maximum distance away from regression location i , called “bandwidth”, which is determined by the number of nearest neighbour points (NNPs).

2.3.2 GWR parameter comparison

To perform the local regression for every local area, the numbers of NNPs are required to estimate spatially varying relationships between CF, AOD and R_s in the GWR-based fused method. To identify the best combination of parameter values, we test the numbers of NNPs ranging from 29 to 1000. Ten percent of merging SunDu-derived R_s data are randomly selected to validate these GWR parameters (**Fig. 1**). The results show that R^2 increases and bias decreases when the number of NNPs decreases. However, when the NNP is smaller than 30, the GWR-based fusion method produces spatially incomplete R_s data due to the local collinearity problem with large spatial variability. Therefore, 30 is selected as the NNP parameter (**Table 3**).

Table 3. Statistical summary of GWR parameter optimization. NPP is the number of nearest neighbour points. GWR-CF presents the GWR-based fused method using only cloud fraction (CF) input, and GWR-CF-AOD presents that of using both CF and aerosol optical depth (AOD) as input. MAB is the mean absolute bias. Std is the standard deviation. RMSE is the root mean square error.

NNP	GWR-CF					GWR-CF-AOD				
	R^2	Bias	MAB	Std	RMSE	R^2	Bias	MAB	Std	RMSE
29	0.91	-0.21	7.45	9.90	9.90	0.91	-0.13	7.47	9.93	9.92
30	0.91	-0.23	7.45	9.90	9.90	0.91	-0.14	7.47	9.92	9.91

31	0.91	-0.24	7.45	9.90	9.90	0.91	-0.14	7.47	9.91	9.91
32	0.91	-0.25	7.46	9.91	9.91	0.91	-0.14	7.47	9.91	9.90
33	0.91	-0.26	7.47	9.92	9.92	0.91	-0.15	7.46	9.90	9.90
34	0.91	-0.27	7.47	9.93	9.93	0.91	-0.14	7.46	9.90	9.89
35	0.91	-0.28	7.48	9.94	9.94	0.91	-0.14	7.46	9.89	9.88
36	0.91	-0.28	7.49	9.94	9.94	0.91	-0.14	7.46	9.89	9.88
37	0.91	-0.29	7.49	9.95	9.95	0.91	-0.14	7.46	9.88	9.87
38	0.91	-0.30	7.50	9.96	9.96	0.91	-0.14	7.46	9.88	9.87
39	0.91	-0.31	7.51	9.98	9.98	0.91	-0.14	7.46	9.87	9.87
40	0.91	-0.32	7.52	9.99	9.99	0.91	-0.14	7.46	9.87	9.87
50	0.90	-0.38	7.62	10.12	10.12	0.91	-0.12	7.51	9.91	9.91
100	0.89	-0.57	8.20	10.90	10.91	0.90	-0.02	7.86	10.31	10.30
500	0.81	-1.08	10.89	14.50	14.54	0.86	0.20	9.55	12.45	12.45
1000	0.75	-1.13	12.60	16.57	16.61	0.82	0.26	10.68	13.84	13.85

3. Results

3.1 Site validation

Based on the independent SunDu validation sites, both the GWR and OLS methods explain 97%~86% of R_s variability (**Fig. 4**). The GWR method generally shows an improved performance compared with the OLS method due to the representativeness of the spatial heterogeneity relationship between R_s and its impact factors in GWR. Both the GWR and OLS methods produce better simulations of R_s if satellite and AOD data are incorporated.

Direct observations from 2000 to 2016 are also used to further evaluate the performance of the fusion methods (**Fig. 4**). The comparative result shows that both fusion methods show slightly reduced performances when using direct R_s observations rather than the SunDu-derived R_s . Both the GWR and OLS methods explain 91%~82% of R_s variability by using direct observations as reference data. Similarly, the GWR method exhibits better performances than the OLS-based fusion method, with an R^2 of 0.91 and root mean square error (RMSE) ranging from 19.89 to 19.97 W/m² at the monthly time scale (**Table 4**).

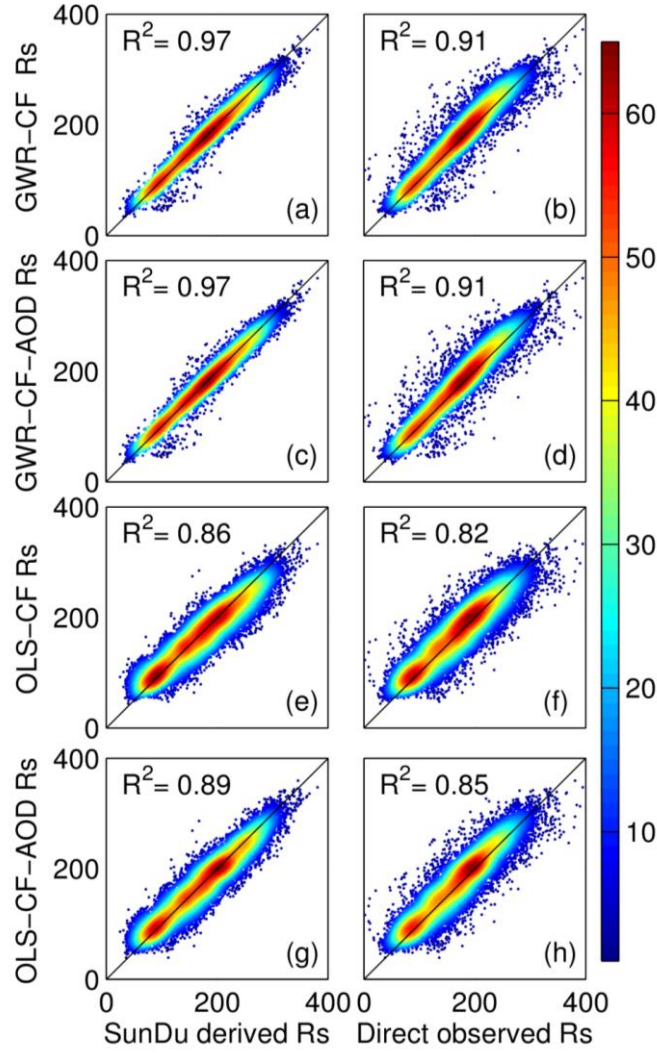


Figure 4. Comparison of surface solar radiation (R_s) derived from the GWR method and the OLS method. Subplots (a, c, e, g) represent validation results using SunDu-derived R_s data as a reference, while that of subplots (b, d, f, h) use directly observed R_s data. Subplots (a, b, c, d) denote the GWR validation results, and subplots (e, f, g, h) denote the OLS validation results.

Table 4. Validation of fusion methods driven by cloud fraction (CF) and AOD. GWR-CF and OLS-CF represent the GWR fusion method and OLS fusion method driven only by CF. GWR-CF-AOD and OLS-CF-AOD represent GWR and OLS fusion methods driven by CF and AOD, respectively.

	Time scale	Ref	R2	Bias	Std	RMSE
GWR-CF	monthly	SunDu R_s	0.97	-1.17	11.41	11.47
GWR-CF-AOD	monthly	SunDu R_s	0.97	-0.82	11.14	11.17
OLS-CF	monthly	SunDu R_s	0.86	-3.80	25.03	25.32
OLS-CF-AOD	monthly	SunDu R_s	0.89	-1.37	22.10	22.15
GWR-CF	monthly	Direct Obs	0.91	4.88	19.29	19.89
GWR-CF-AOD	monthly	Direct Obs	0.91	5.24	19.27	19.97
OLS-CF	monthly	Direct Obs	0.82	2.18	26.73	26.82
OLS-CF-AOD	monthly	Direct Obs	0.85	4.64	24.71	25.15
GWR-CF	spring	SunDu R_s	0.95	-1.3	11.5	11.57
GWR-CF-AOD	spring	SunDu R_s	0.95	-0.86	11.2	11.23
OLS-CF	spring	SunDu R_s	0.77	-4.97	23.65	24.16
OLS-CF-AOD	spring	SunDu R_s	0.84	-1.35	19.85	19.9
GWR-CF	summer	SunDu R_s	0.9	-2.09	14.08	14.23
GWR-CF-AOD	summer	SunDu R_s	0.9	-1.38	13.76	13.82
OLS-CF	summer	SunDu R_s	0.65	-6.49	26.18	26.97
OLS-CF-AOD	summer	SunDu R_s	0.77	-1.37	21.17	21.22
GWR-CF	autumn	SunDu R_s	0.95	-1.27	9.48	9.56
GWR-CF-AOD	autumn	SunDu R_s	0.96	-1.04	9.17	9.23
OLS-CF	autumn	SunDu R_s	0.67	-3.22	25.62	25.82
OLS-CF-AOD	autumn	SunDu R_s	0.71	-1.97	23.79	23.87
GWR-CF	winter	SunDu R_s	0.94	0.01	9.87	9.86
GWR-CF-AOD	winter	SunDu R_s	0.94	0.04	9.78	9.78
OLS-CF	winter	SunDu R_s	0.63	-0.37	24.16	24.16
OLS-CF-AOD	winter	SunDu R_s	0.65	-0.78	23.41	23.42
GWR-CF	annual	Direct Obs	0.37	5.62	4.73	10.42
GWR-CF-AOD	annual	Direct Obs	0.37	5.98	4.79	10.53
OLS-CF	annual	Direct Obs	0.30	3.06	5.01	15.01
OLS-CF-AOD	annual	Direct Obs	0.33	5.45	4.89	13.34
GWR-CF	annual	SunDu R_s	0.57	-1.19	4.30	6.76
GWR-CF-AOD	annual	SunDu R_s	0.58	-0.84	4.30	6.68
OLS-CF	annual	SunDu R_s	0.35	-3.58	5.63	15.17
OLS-CF-AOD	annual	SunDu R_s	0.39	-1.23	5.44	13.40
GWR-CF	annual mean	SunDu R_s	0.94	-1.50	6.63	6.76
GWR-CF-AOD	annual mean	SunDu R_s	0.95	-1.15	6.41	6.47
OLS-CF	annual mean	SunDu R_s	0.62	-3.90	17.11	17.46
OLS-CF-AOD	annual mean	SunDu R_s	0.71	-1.58	14.90	14.90
GWR-CF	annual mean	Direct Obs	0.89	5.08	9.85	11.03
GWR-CF-AOD	annual mean	Direct Obs	0.89	5.43	9.75	11.11
OLS-CF	annual mean	Direct Obs	0.70	2.57	16.31	16.42
OLS-CF-AOD	annual mean	Direct Obs	0.77	4.88	14.00	14.75

3.2 Seasonal and annual variations in R_s

To analyse the impacts of AOD on the GWR fusion results, the GWR driven with only CF (GWR-CF) and GWR driven with CF and AOD (GWR-CF-AOD) are compared. Two validation sites (Chang Chun, 43.87°N 125.33°E and Bei Hai, 21.72°N

109.08°E) are randomly selected to evaluate the seasonal and annual variations in R_s derived from the GWR method (Fig. 5). The multiyear mean of AOD from Changchun and BeiHai are 0.49 and 0.70, respectively. As shown in subplots (a and b), both GWR-CF and GWR-CF-AOD produce similar seasonal variation patterns compared with SunDu-derived R_s and CERES EBAF R_s data. Small differences are found in the seasonal variation in R_s derived from GWR regardless of whether AOD was incorporated. Examination of the annual variation R_s from the GWR-CF and GWR-CF-AOD are shown in subplots (c and d) of Figure 5. The two fusion methods also produce similar annual R_s variations. The similar performances of the GWR-CF and GWR-CF-AOD might suggest that the impacts of AOD have already been included in the SunDu-derived R_s site data.

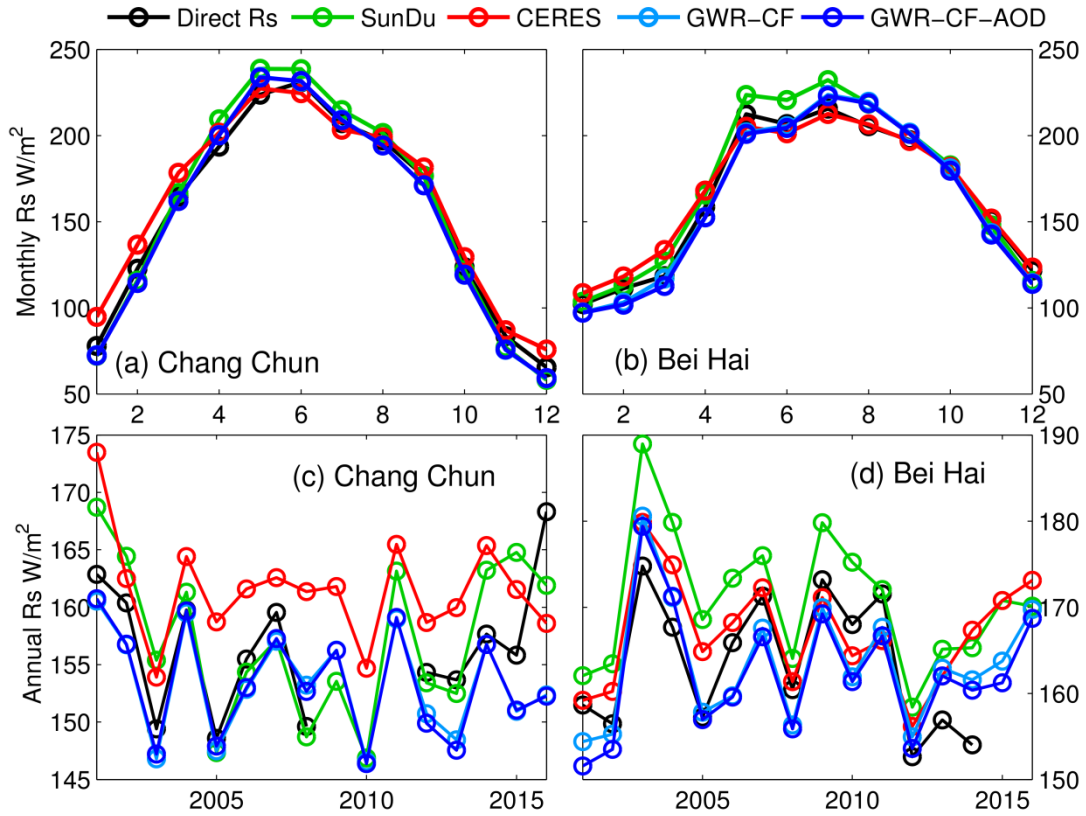


Figure 5. Seasonal and annual variations in R_s at two sites: Chang Chun (a and c, 43.87°N and 125.33°E) and Bei Hai (b and d, 23.50°N, 99.72°E). SunDu R_s is the SunDu-derived R_s data, and GWR-CF R_s is R_s produced by the GWR method

incorporating only the cloud fraction. GWR-CF-AOD is R_s produced by the GWR method incorporating cloud fraction and AOD. The multiyear mean of AOD from Changchun and BeiHai are 0.49 and 0.70, respectively.

We also analyse the performances of fusion methods for different seasons at all validation sites, as shown in **Table 4**. At seasonal scales, both the GWR-CF and GWR-CF-AOD methods have high R^2 values ranging from 0.94 to 0.96, compared with direct R_s measurement or SunDu-derived R_s . GWR-CF and GWR-CF-AOD show slight differences, indicating that both fusion methods produce consistent R_s seasonal variation patterns, which might be because the impacts of AOD have already been included in the SunDu-derived R_s site data at seasonal time scales. Comparatively, the GWR methods perform best in autumn, with RMSEs ranging from 9.23W/m² to 9.56 W/m² followed by winter, spring and summer. Both the GWR-CF and GWR-CF-AOD methods produce similar annual variations in R_s from 2000 to 2016, with R^2 values ranging from 0.57 to 0.58 (**Table 4**). The statistics indicate that the GWR can produce reasonable seasonal and annual variations in R_s .

3.3 Multiyear mean and long-term variability in R_s

Figure 6 shows the performance of GWR-CF and GWR-CF-AOD on simulating the multiyear mean R_s by using 97 direct R_s observation sites and independent SunDu-derived R_s sites. Based on direct R_s measurements, both GWR-based methods show good performances with high R^2 (0.89~0.95) and low RMSE (11.03~11.11 W/m²), and few differences are found for the GWR merging results, whether or not AOD is taken as input data (**Table 4**).

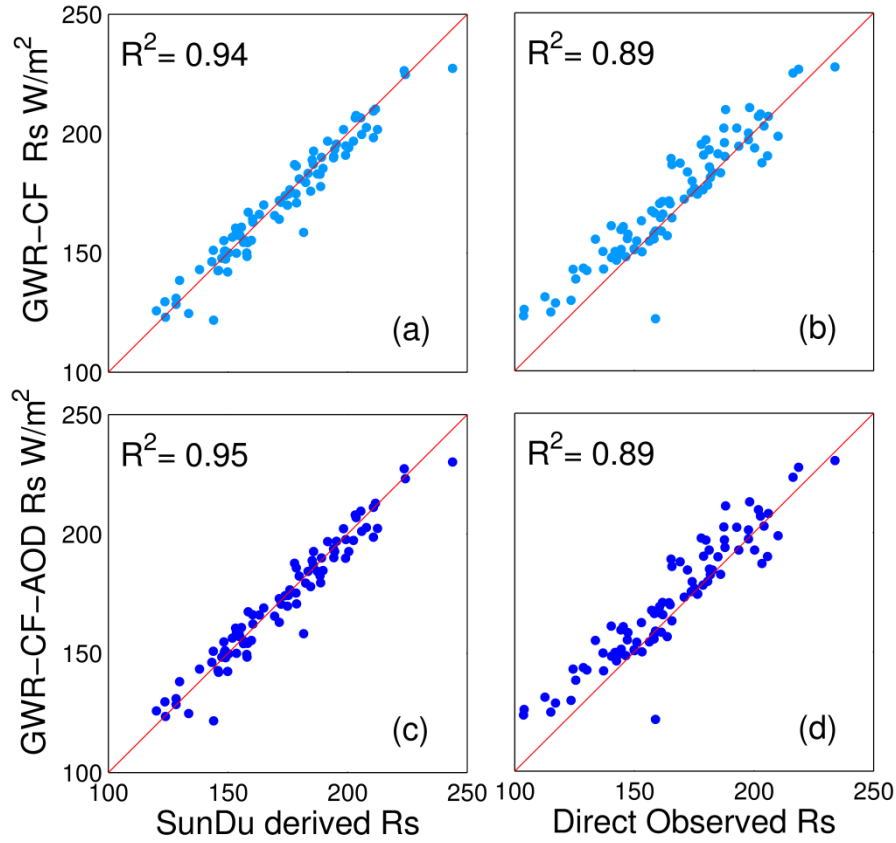


Figure 6. Comparison of multiyear mean surface solar radiation (R_s) derived from the GWR method. Subplots (a, c) represent validation results using SunDu-derived R_s data as a reference, while that of subplots (b, d) use direct observed R_s data.

The spatial distributions of the multiyear means of R_s from 2000 to 2017 are shown in **Figure 7**. The SunDu sites show that R_s is high in northwest China, ranging from 180 to 300 W/m², and low in eastern China, ranging from 120 to 180 W/m². Both the GWR-CF and GWR-CF-AOD methods show consistent R_s spatial patterns with SunDu-derived R_s observations and CERES EBAFs, indicating that the relationship between R_s and impact factors is not linearly stable and is closely related to spatial position. The spatial distribution of the R_s trend derived from the GWR method is also consistent with the SunDu-derived R_s trend, especially in western China (**Fig. 8**).

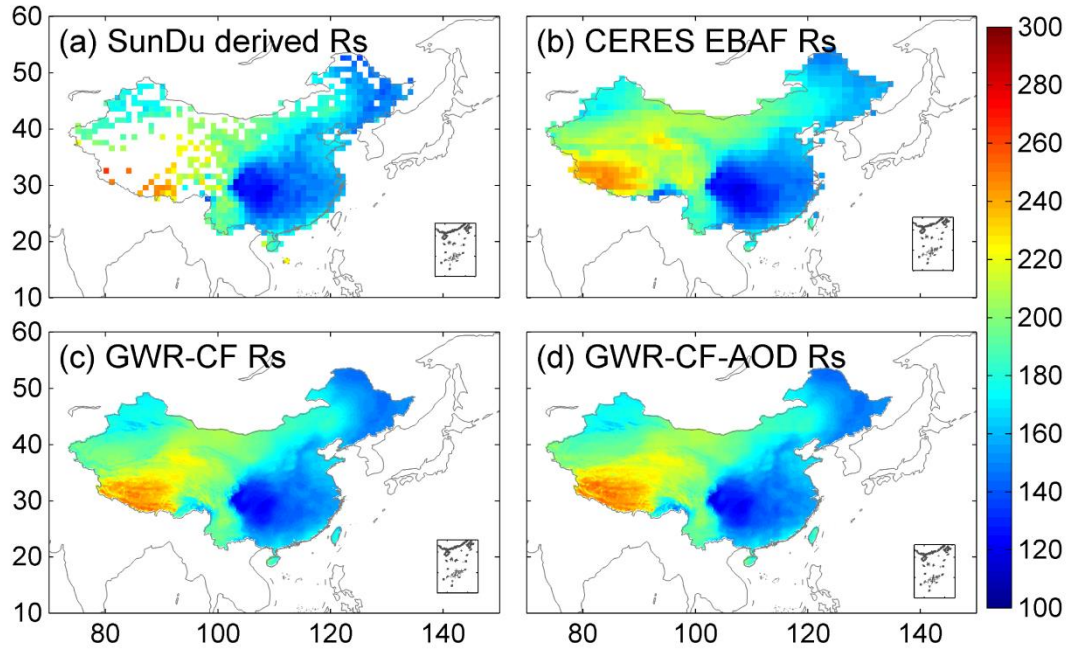


Figure 7. Spatial distribution of multiyear mean monthly surface solar radiation (R_s) from 2000 to 2017. The first line (a, b) shows the observed multiyear mean monthly R_s from SunDu and CERES EBAF; the multiyear mean monthly R_s derived from the GWR method are shown in the second line (c, d), respectively.

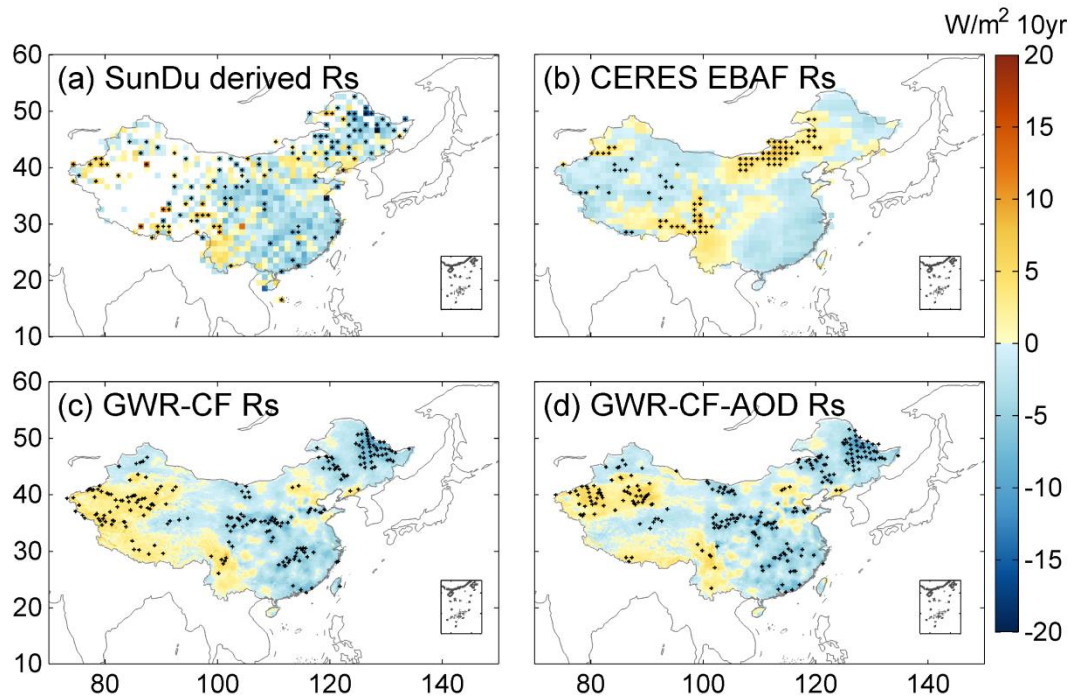


Figure 8. Spatial distributions of monthly anomaly trends of surface solar radiation (R_s) from 2000 to 2017. The first line (a, b) shows the SunDu-derived R_s and CERES EBAF

R_s ; the R_s -derived GWR fusion methods are shown in the second line (c, d). Subplots (c) incorporate only CF, and subplots (d) incorporate CF and AOD. The black dots on the maps represent significant trends ($P < 0.05$).

Based on the classified subregions using 97 direct R_s observations in **Figure 1**, the regional means of R_s annual anomaly variation from 2000 to 2016 are shown in **Figure 9**. Compared with observations, both the GWR-CF and GWR-CF-AOD methods produce consistent long-term R_s trends with SunDu-derived R_s and CERES EBAF R_s (**Figures 2, 3 and 9**), indicating that the GWR-CF and GWR-CF-AOD methods can produce reasonable annual R_s variations over China.

In zones I and II, located in northern arid/semiarid regions, the annual anomaly R_s variation shows small fluctuations ranging from -10 to 10 W/m². In contrast, zones IV, V, VIII and IX covering the Sichuan Basin, Yunnan-Guizhu Plateau, Qinghai-Tibet Plateau and North China Plain show large R_s variation trends. Li et al. (2018) found a sharply increasing R_s trend over East China, especially in the North China Plain, which is due to controlling air pollution and reducing aerosol loading. However, our results indicate that the increased surface solar radiation in North China is not confirmed by satellite retrieval (CERES) and SunDu-derived R_s .

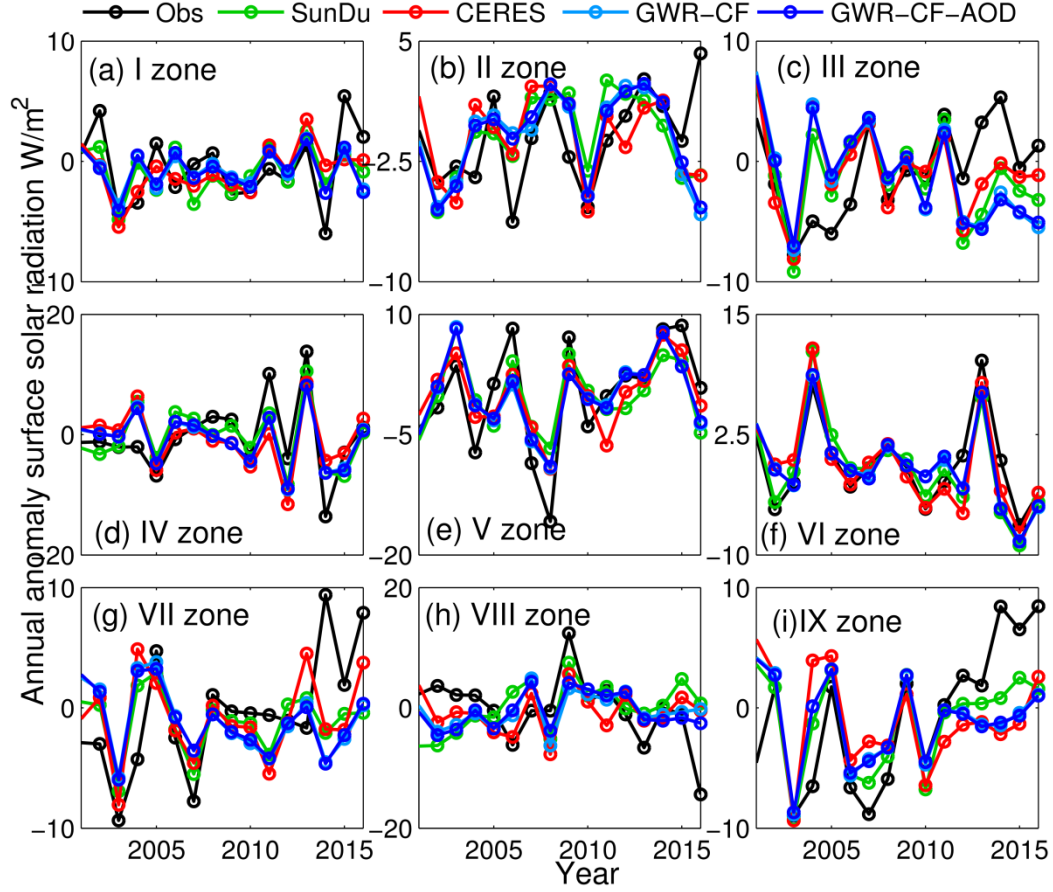


Figure 9. The regional mean of the annual anomaly of the surface solar radiation (R_s) for different subregions. Nine subregions (I to IX) over China are shown in Figure 1. Direct R_s observations, SunDu-derived R_s , and CERES EBAF are shown as black lines, green lines and red lines, respectively. Light and dark blue represent the R_s variation derived from the GWR-CF and the GWR-CF-AOD methods.

4. Discussion

4.1 Impact factors of R_s

In this study, we merged more than 2400 sunshine duration-derived R_s site data with MODIS CF and AOD data to generate high spatial resolution (0.1°) R_s over China from 2000 to 2017. The results show that the GWR method incorporated with CF and

AOD (GWR-CF-AOD) performs best, indicating the non-neglected role of clouds and aerosols in regulating the variation in R_s over China.

Clouds and aerosols impact the solar radiation reaching the surface by radiative absorption and scattering (Tang et al., 2017). Recent R_s trend studies over Europe suggest that CF may play a key role in the positive trend of R_s since the 1990s (Pfeifroth et al., 2018a). In terms of input data, our results also indicate that the cloud fraction might be a major factor affecting R_s , which is consistent with our previous studies (Feng and Wang, 2019).

Changes in aerosol loading have also been reported to be an important impact factor (Che et al., 2005; Li et al., 2018; Liang and Xia, 2005; Qian et al., 2015; Xia, 2010; Zhou et al., 2019b). The atmospheric visibility data show that the slope of the linear variation in surface solar radiation with respect to atmospheric visibility is distinctly different at different stations (Yang et al., 2017), implying that the relationship between R_s and aerosols varies with location.

4.2 Performances of the fusion methods

The good overall performances of the GWR model have been reported in many previous studies, including geography (Chao et al., 2018; Georganos et al., 2017), economics (Ma and Gopal, 2018), meteorology (Li and Meng, 2017; Zhou et al., 2019a), and epidemiology (Tsai and Teng, 2016). Chao et al. (2018) used the GWR method to merge satellite precipitation and gauge observations to correct biases in satellite precipitation data and downscale satellite precipitation to a finer spatial resolution at the same time. Zhou et al. (2019a) used GWR to analyse haze pollution over China and found that the GWR estimate was better than the OLS estimate, with an improvement in correlation coefficient from 0.20 to 0.75.

Compared with other traditional interpolation methods, such as optimal

interpolation (OI), GWR can theoretically integrate geographical location and R_s impact factors for spatial R_s estimations and reflect the non-stationary spatial relationship between R_s and its impact factors. The thin plate spline method can include CF and AOD as covariates to simulate the approximately linear dependence of these impact factors on R_s , but this linear function cannot fully describe the relationship among CF, AOD and R_s (Hong et al., 2005).

Comparison results from (Wang et al., 2017) also indicate that the GWR method is better than the multiple linear regression method and spline interpolation method for near surface air temperature. By using spatial interpolation method, CERES EBAF R_s can also be downscaled to 1km or 30m. These interpolated CERES R_s data cannot represent the detailed R_s distributions at spatial resolution of 1km or 30m due to the variability of R_s within a 1 degree box. Without additional high spatial resolution data, interpolated cannot capture more detail variability of R_s .

5. Data availability

The merged R_s product by GWR methods with cloud fraction and AOD data as input in this study are available at <https://doi.pangaea.de/10.1594/PANGAEA.921847> (Feng and Wang, 2020).

6. Conclusions

Accurate estimation of R_s variability is crucially important for regional energy budget, water cycle and climate change studies. Recent studies have shown that SunDu-derived R_s data can provide reliable long-term R_s series. In this study, we merged SunDu-derived R_s data with satellite-derived cloud fraction (CF) and aerosol optical

depth (AOD) data to generate high spatial resolution (0.1°) R_s over China from 2000 to 2017 (Feng and Wang, 2020). The GWR and OLS merging methods were also compared.

Our results show that the spatial resolutions of all fusion results are improved to 0.1° by incorporating MODIS cloud fraction data. The GWR shows better performance than OLS, with increases in R^2 by 9.21%~12.81% and RMSEs reduced by 49.56%~54.68%, indicating that R_s has complex characteristics of spatial variability over China, which has also indicated the necessity of the high spatial resolution of R_s data. As clouds and aerosols play vital roles in the variability in R_s , apparent improvements in the results of SunDu-derived R_s data merging are found if both cloud fraction and AOD are incorporated. Based on the merging results incorporating only cloud fraction, cloud fraction is suggested to be the major factor impacting R_s , which explained approximately 86%~97% of R_s variability. Generally, SunDu-derived R_s data merging results derived from GWR show more consistent multiyear mean R_s and long-term R_s trends compared with those from OLS. Our results show that the improvement in R_s variability estimation is closely related to R_s impact factors and R_s spatial heterogeneity. The merged R_s products derived from GWR-CF-AOD can be downloaded at <https://doi.pangaea.de/10.1594/PANGAEA.921847>.

Acknowledgements

This study was funded by the National Key Research & Development Program of China (2017YFA06036001), the National Natural Science Foundation of China (41525018), the Fundamental Research Funds for the Central Universities (#BLX201907), and the State Key Laboratory of Earth Surface Processes and Resource Ecology (U2020-KF-02). We would like to thank Chengyang Xu, Yuna Mao, Jizeng Du,

579 Runze Li, Qian Ma, Guocan Wu, and Chunlue Zhou for their insightful comments. We
580 are grateful to Amelie Driemel for her help of uploading the data in PANGAEA. The
581 cloud data can be downloaded from
582 https://neo.sci.gsfc.nasa.gov/view.php?datasetId=MODAL2_M_CLD_FR. The
583 CERES SYN data can be downloaded from <https://ceres.larc.nasa.gov/data/>.

584

585

References

- Ali, K., Partridge, M. D., and Olfert, M. R.: Can Geographically Weighted Regressions Improve Regional Analysis and Policy Making?, *Int. Reg. Sci. Rev.*, 30, 300-329, 2007.
- Brunsdon, C., Fotheringham, A. S., and Charlton, M. E.: Geographically Weighted Regression : A Method for Exploring Spatial Nonstationarity, *geographical analysis*, 28, 281-298, 2010.
- Brunsdon, C., Fotheringham, S., and Charlton, M.: Geographically Weighted Regression. 1998.
- Camargo, L. R. and Dorner, W.: Integrating satellite imagery derived data and GIS-based solar radiation algorithms to map solar radiation in high temporal and spatial resolutions for the province of Salta, Argentina, *SPIE Remote Sensing*, 100050E, 2016.
- Chao, L., Zhang, K., Li, Z., Zhu, Y., Wang, J., and Yu, Z.: Geographically weighted regression based methods for merging satellite and gauge precipitation, *J. Hydrol.*, 558, 275-289, 2018.
- Che, H. Z., Shi, G. Y., Zhang, X. Y., Arimoto, R., Zhao, J. Q., Xu, L., Wang, B., and Chen, Z. H.: Analysis of 40 years of solar radiation data from China, 1961–2000, *Geophys. Res. Lett.*, 1029, 2341-2352, 2005.
- Collins, W. D., Rasch, P. J., Eaton, B. E., Khattatov, B. V., Lamarque, J. F., and Zender, C. S.: Simulating aerosols using a chemical transport model with assimilation of satellite aerosol retrievals: Methodology for INDOEX, *J. Geophys. Res.*, 106, 7313-7336, 2001.
- Cornejo-Bueno, L., Casanova-Mateo, C., Sanz-Justo, J., and Salcedo-Sanz, S.: Machine learning regressors for solar radiation estimation from satellite data, *Sol. Energy*,

183, 768-775, 2019.

Dai, A., Karl, T. R., Sun, B., and Trenberth, K. E.: Recent Trends in Cloudiness over the United States: A Tale of Monitoring Inadequacies, *Bull. Am. Meteorol. Soc.*, 87, 597-606, 2006.

Doelling, D. R., Loeb, N. G., Keyes, D. F., Nordeen, M. L., Morstad, D., Nguyen, C., Wielicki, B. A., Young, D. F., and Sun, M.: Geostationary Enhanced Temporal Interpolation for CERES Flux Products, *J. Atmos. Ocean Technol.*, 30, 1072-1090, 2013.

Evan, A. T., Heidinger, A. K., and Vimont, D. J.: Arguments against a physical long-term trend in global ISCCP cloud amounts, *Geophys. Res. Lett.*, 34, 290-303, 2007.

Feng, F. and Wang, K.C.: Determining Factors of Monthly to Decadal Variability in Surface Solar Radiation in China: Evidences From Current Reanalyses, *J. Geophys. Res. Atmos.*, 124, 9161-9182, 2019.

Feng, F. and Wang, K. C.: Merging Satellite Retrievals and Reanalyses to Produce Global Long-Term and Consistent Surface Incident Solar Radiation Datasets, *Remote Sens.*, 10, 115, 2018.

Feng, F. and Wang, K. C.: Monthly surface solar radiation data over China (2000-2017) by merging satellite cloud and aerosol data with ground-based sunshine duration data. PANGAEA, <https://doi.pangaea.de/10.1594/PANGAEA.921847>, 2020.

Feng, Y., Chen, D., and Zhao, X.: Estimated long-term variability of direct and diffuse solar radiation in North China during 1959–2016, *Theor. Appl. Climatol.*, 137, 153-163, 2019.

Fotheringham, A. S., Charlton, M., and Brunson, C.: The geography of parameter space: an investigation of spatial non-stationarity, *Int. J. Geogr. Inf. Syst.*, 10, 605-627, 1996.

636 Gao, X., Asami, Y., and Chung, C.-J. F.: An empirical evaluation of spatial regression
637 models, *Comput. Geosci.*, 32, 1040-1051, 2006.

638 Georganos, S., Abdi, A. M., Tenenbaum, D. E., and Kalogirou, S.: Examining the
639 NDVI-rainfall relationship in the semi-arid Sahel using geographically weighted
640 regression, *J. Arid Environ.*, 146, 64-74, 2017.

641 Hakuba, M. Z., Folini, D., Schaepman-Strub, G., and Wild, M.: Solar absorption over
642 Europe from collocated surface and satellite observations, *J. Geophys. Res.*, 119,
643 3420-3437, 2014.

644 He, Y., Wang, K., Zhou, C., and Wild, M.: A Revisit of Global Dimming and
645 Brightening Based on the Sunshine Duration, *Geophys. Res. Lett.*, 45(9), 4281-
646 4289, 2018.

647 He, Y. and Wang, K. C.: Variability in direct and diffuse solar radiation across China
648 from 1958 to 2017, *Geophys. Res. Lett.*, 47, 2020.

649 Hong, Y., Nix, H. A., Hutchinson, M. F., and Booth, T. H.: Spatial interpolation of
650 monthly mean climate data for China, *Int. J. Climatol.*, 25, 1369-1379, 2005.

651 Hongrong, S., Weiwei, L., Xuehua, F., Jinqiang, Z., Bo, H., Letu, H., Huazhe, S., Xinlei,
652 H., Zijue, S., and Yingjie, Z.: First assessment of surface solar irradiance derived
653 from Himawari-8 across China, *Sol. Energy*, 174, 164-170, 2018.

654 Hou, N., Zhang, X., Zhang, W., Xu, J., Feng, C., Yang, S., Jia, K., Yao, Y., Cheng, J.,
655 and Jiang, B.: A New Long-Term Downward Surface Solar Radiation Dataset over
656 China from 1958 to 2015, *Sensors (Basel)*, 20, 2020.

657 Huang, G., Li, Z., Li, X., Liang, S., Yang, K., Wang, D., and Zhang, Y.: Estimating
658 surface solar irradiance from satellites: Past, present, and future perspectives,
659 *Remote Sens. Environ.*, 233, 111371, 2019.

660 Jia, B., Xie, Z., Dai, A., Shi, C., and Chen, F.: Evaluation of satellite and reanalysis

661 products of downward surface solar radiation over East Asia: Spatial and seasonal
662 variations, *J. Geophys. Res. Atmos.*, 118, 3431-3446, 2013.

663 Jin, H.-a., Li, A.-n., Bian, J.-h., Zhang, Z.-j., Huang, C.-q., and Li, M.-x.: Validation of
664 global land surface satellite (GLASS) downward shortwave radiation product in
665 the rugged surface, *J Mt. Sci.*, 10, 812-823, 2013.

666 Jin, Z., Yezheng, W., and Gang, Y.: General formula for estimation of monthly average
667 daily global solar radiation in China, *Energy Convers.Manag.*, 46, 257-268, 2005.

668 Journée, M. and Bertrand, C.: Improving the spatio-temporal distribution of surface
669 solar radiation data by merging ground and satellite measurements, *Remote Sens.*
670 *Environ.*, 114, 2692-2704, 2010.

671 Journée, M., Müller, R., and Bertrand, C.: Solar resource assessment in the Benelux by
672 merging Meteosat-derived climate data and ground measurements, *Sol. Energy*, 86,
673 3561-3574, 2012.

674 Karlsson, K.-G., Anttila, K., Trentmann, J., Stengel, M., Meirink, J. F., Devasthale, A.,
675 Hanschmann, T., Kothe, S., Jääskeläinen, E., and Sedlar, J.: CLARA-A2: the
676 second edition of the CM SAF cloud and radiation data record from 34 years of
677 global AVHRR data, *Atmos. Chem. Phys.*, 17, 1-41, 2017.

678 Kato, S., Rose, F. G., Rutan, D. A., Thorsen, T. J., Loeb, N. G., Doelling, D. R., Huang,
679 X., Smith, W. L., Su, W., and Ham, S.-H.: Surface Irradiances of Edition 4.0
680 Clouds and the Earth's Radiant Energy System (CERES) Energy Balanced and
681 Filled (EBAF) Data Product, *J. Clim.*, 31, 4501-4527, 2018.

682 Leckner, B. G.: The spectral distribution of solar radiation at the earth's surface—
683 elements of a model, *Sol. Energy*, 20, 143-150, 1978.

684 LeSage, J. P.: *A Family of Geographically Weighted Regression Models*. 2004.

685 Letu, H., Yang, K., Nakajima, T. Y., Ishimoto, H., Nagao, T. M., Riedi, J., Baran, A. J.,

686 Ma, R., Wang, T., Shang, H., Khatri, P., Chen, L., Shi, C., and Shi, J.: High-
687 resolution retrieval of cloud microphysical properties and surface solar radiation
688 using Himawari-8/AHI next-generation geostationary satellite, *Remote Sens.*
689 *Environ.*, 239, 111583, 2020.

690 Li, J., Jiang, Y. W., Xia, X. G., and Hu, Y. Y.: Increase of surface solar irradiance across
691 East China related to changes in aerosol properties during the past decade,
692 *Environ.Res. Lett.*, 13, 034006, 2018.

693 Li, T. and Meng, Q.: Forest dynamics to precipitation and temperature in the Gulf of
694 Mexico coastal region, *Int. J. Biometeorol.*, 61, 869-879, 2017.

695 Liang, F. and Xia, X. A.: Long-term trends in solar radiation and the associated climatic
696 factors over China for 1961-2000, *Annales Geophysicae*, 23, 2425-2432, 2005.

697 Loghmari, I., Timoumi, Y., and Messadi, A.: Performance comparison of two global
698 solar radiation models for spatial interpolation purposes, *Renew.Sust. Energ. Rev.*,
699 82, 837-844, 2018.

700 Lorenzo, A. T., Morzfeld, M., Holmgren, W. F., and Cronin, A. D.: Optimal
701 interpolation of satellite and ground data for irradiance nowcasting at city scales,
702 *Sol. Energy*, 144, 466-474, 2017.

703 Lu, W., Mo, Y., and Wang, D.: Characteristics investigation for pyranometers, *Acta*
704 *Energi. Sin.*, 23, 313–316, 2002.

705 Lu, W. H. and Bian, Z. Q.: Station experiment and preliminary data analysis of high-
706 precision solar radiation measurement system, *Meteorol. Hydrol. Mar. Instrum.*, 3,
707 1-5, 2012.

708 Luo, Y., Lu, D., Zhou, X., Li, W., and He, Q.: Characteristics of the spatial distribution
709 and yearly variation of aerosol optical depth over China in last 30 years, *J.*
710 *Geophys. Res.*, 106, 14501-14513, 2001.

711 Ma, Q., Wang, K. C., and Wild, M.: Impact of geolocations of validation data on the
712 evaluation of surface incident shortwave radiation from Earth System Models, J.
713 Geophys. Res. Atmos., 120, 6825-6844, 2015.

714 Ma, Y. and Gopal, S.: Geographically Weighted Regression Models in Estimating
715 Median Home Prices in Towns of Massachusetts Based on an Urban Sustainability
716 Framework, Sustainability, 10, 1026, 2018.

717 Manara, V., Beltrano, M. C., Brunetti, M., Maugeri, M., Sanchez-Lorenzo, A., Simolo,
718 C., and Sorrenti, S.: Sunshine duration variability and trends in Italy from
719 homogenized instrumental time series (1936–2013), J. Geophys. Res. Atmos., 120,
720 3622-3641, 2015.

721 Manara, V., Brunetti, M., Maugeri, M., Sanchez-Lorenzo, A., and Wild, M.: Sunshine
722 duration and global radiation trends in Italy (1959–2013): To what extent do they
723 agree?, J. Geophys. Res., 122, 4312-4331, 2017.

724 Mo, Y. Q., Yang, Y., Liang, H. L., and Wang, D.: Investigation report on technology of
725 status and development of meteorological radiation observation in China, Chinese
726 J. Sci. Instrum., 29, 518–522, 2008.

727 Montero-Martín, J., Antón, M., Vaquero-Martínez, J., and Sanchez-Lorenzo, A.:
728 Comparison of long-term solar radiation trends from CM SAF satellite products
729 with ground-based data at the Iberian Peninsula for the period 1985–2015, Atmos.
730 Res., 236, 104839, 2020.

731 Myers, D. R.: Solar radiation modeling and measurements for renewable energy
732 applications: data and model quality, Energy, 30, 1517-1531, 2005.

733 Pfeifroth, U., Bojanowski, J. S., Clerbaux, N., Manara, V., Sanchez-Lorenzo, A.,
734 Trentmann, J., Walawender, J. P., Hollmann, R., and Jakub, W. P.: Satellite-based
735 trends of solar radiation and cloud parameters in Europe, Adv. Sci. Res., 15, 31-

37, 2018a.

Pfeifroth, U., Sanchez-Lorenzo, A., Manara, V., Trentmann, J., and Hollmann, R.: Trends and Variability of Surface Solar Radiation in Europe Based On Surface and Satellite-Based Data Records, *J. Geophys. Res. Atmos.*, 123, 1735–1754, 2018b.

Platnick, S., Ackerman, S., King, M., Wind, G., Meyer, K., Menzel, W., Holz, R., Baum, B., and Yang, P.: MODIS atmosphere L2 cloud product (06_L2), NASA MODIS Adaptive Processing System, Goddard Space Flight Center, 1, 1, 2017.

Qian, Y., Kaiser, D. P., Leung, L. R., and Xu, M.: More frequent cloud-free sky and less surface solar radiation in China from 1955 to 2000, *Geophys. Res. Lett.*, 33, 311-330, 2015.

Rahman, M. and Zhang, W.: Review on estimation methods of the Earth's surface energy balance components from ground and satellite measurements, *J Earth Syst. Sci.*, 128, 2019.

Ruiz-Arias, J. A., Quesada-Ruiz, S., Fernández, E. F., and Gueymard, C. A.: Optimal combination of gridded and ground-observed solar radiation data for regional solar resource assessment, *Sol. Energy*, 112, 411-424, 2015.

Rutan, D. A., Kato, S., Doelling, D. R., Rose, F. G., Nguyen, L. T., Caldwell, T. E., and Loeb, N. G.: CERES Synoptic Product: Methodology and Validation of Surface Radiant Flux, *J. Atmos. Ocean Technol.*, 32, 1121-1143, 2015.

Sanchezlorenzo, A., Azorinmolina, C., Wild, M., Vicenteserrano, S. M., Lópezmoreno, J. I., and Corellcustardoy, D.: Feasibility of sunshine duration records to detect changes in atmospheric turbidity: A case study in Valencia (Spain), *AIP Conf. Proc.*, 736-739, 2013.

Sanchezlorenzo, A., Calbó, J., Brunetti, M., and Deser, C.: Dimming/brightening over the Iberian Peninsula: Trends in sunshine duration and cloud cover and their

relations with atmospheric circulation, *J. Geophys. Res. Atmos.*, 114, 114, D100D109, doi:10.1029/2008JD011394., 2009.

Sanchezromero, A., Sanchezlorenzo, A., Calbó, J., González, J. A., and Azorin-Molina, C.: The signal of aerosol-induced changes in sunshine duration records: A review of the evidence, *J. Geophys. Res. Atmos.*, 119, 4657–4467, 2014.

Schwarz, M., Folini, D., Yang, S., Allan, R. P., and Wild, M.: Changes in atmospheric shortwave absorption as important driver of dimming and brightening, *Nat. Geosci.*, 13, 110-115, 2020.

Sheehan, K. R., Strager, M. P., and Welsh, S. A.: Advantages of Geographically Weighted Regression for Modeling Benthic Substrate in Two Greater Yellowstone Ecosystem Streams, *Environ. Monit. Assess.*, 18, 209-219, 2012.

Shi, G.-Y., Hayasaka, T., Ohmura, A., Chen, Z.-H., Wang, B., Zhao, J.-Q., Che, H.-Z., and Xu, L.: Data Quality Assessment and the Long-Term Trend of Ground Solar Radiation in China, *J. Appl. Meteorol. Climatol.*, 47, 1006-1016, 2008.

Stengel, M., Stapelberg, S., Sus, O., Finkensieper, S., Würzler, B., Philipp, D., Hollmann, R., Poulsen, C., Christensen, M., and McGarragh, G.: Cloud_cci Advanced Very High Resolution Radiometer post meridiem (AVHRR-PM) dataset version 3: 35-year climatology of global cloud and radiation properties, *Earth Syst. Sci. Data*, 12, 41-60, 2020.

Tang, W., Yang, K., Qin, J., Li, X., and Niu, X.: A 16-year dataset (2000–2015) of high-resolution (3 h, 10 km) global surface solar radiation, *Earth Syst. Sci. Data*, 11, 1905-1915, 2019.

Tang, W., Yang, K., Qin, J., Niu, X., Lin, C., and Jing, X.: A revisit to decadal change of aerosol optical depth and its impact on global radiation over China, *Atmospheric Environment*, 150, 106e115, 2017.

786 Tang, W. J., Yang, K., Qin, J., Cheng, C. C. K., and He, J.: Solar radiation trend across
787 China in recent decades: a revisit with quality-controlled data, *Atmos. Chem. Phys.*,
788 11, 393-406, 2011.

789 Tsai, P. and Teng, H.: Role of *Aedes aegypti* (Linnaeus) and *Aedes albopictus* (Skuse)
790 in local dengue epidemics in Taiwan, *BMC Infectious Diseases*, 16, 662, 2016.

791 Wang, K. C.: Measurement biases explain discrepancies between the observed and
792 simulated decadal variability of surface incident solar radiation, *Sci. Rep.*, 4, 6144,
793 2014.

794 Wang, K. C. and Dickinson, R. E.: Contribution of solar radiation to decadal
795 temperature variability over land, *Proc. Natl. Acad. Sci. U.S.A.*, 110, 14877, 2013.

796 Wang, K. C., Ye, H., Chen, F., Xiong, Y., and Wang, C.: Urbanization Effect on the
797 Diurnal Temperature Range: Different Roles under Solar Dimming and
798 Brightening*, *J. Clim.*, 25, 1022-1027, 2012a.

799 Wang, K. C., Ma, Q., Li, Z., and Wang, J.: Decadal variability of surface incident solar
800 radiation over China: Observations, satellite retrievals, and reanalyses, *J. Geophys.*
801 *Res. Atmos.*, 120, 6500-6514, 2015.

802 Wang, M., He, G., Zhang, Z., Wang, G., Zhang, Z., Cao, X., Wu, Z., and Liu, X.:
803 Comparison of Spatial Interpolation and Regression Analysis Models for an
804 Estimation of Monthly Near Surface Air Temperature in China, *Remote Sens.*, 9,
805 1278, 2017.

806 Wang, Y., Yang, Y., Zhao, N., Liu, C., and Wang, Q.: The magnitude of the effect of air
807 pollution on sunshine hours in China, *J. Geophys. Res. Atmos.*, 117, 116-116, 2012b.

808 Wei, Y., Zhang, X., Hou, N., Zhang, W., Jia, K., and Yao, Y.: Estimation of surface
809 downward shortwave radiation over China from AVHRR data based on four
810 machine learning methods, *Sol. Energy*, 177, 32-46, 2019.

811 Wild, M.: Decadal changes in radiative fluxes at land and ocean surfaces and their
812 relevance for global warming, *Wiley Interdisciplinary Reviews Climate Change*,
813 7, 91-107, 2016.

814 Wild, M.: Global dimming and brightening: A review, *J. Geophys. Res. Atmos.*, 114,
815 D00D16, 2009.

816 Wild, M.: Towards Global Estimates of the Surface Energy Budget, *Curr. Clim. Change*
817 *Rep.*, 2017. 1-11, 2017.

818 Xia, X.: Spatiotemporal changes in sunshine duration and cloud amount as well as their
819 relationship in China during 1954–2005, *J. Geophys. Res. Atmos.*, 115, 86, 2010.

820 Yang, H., Li, Z., Li, M., and Yang, D.: Inconsistency in Chinese solar radiation data
821 caused by instrument replacement: Quantification based on pan evaporation
822 observations, *J. Geophys. Res.*, 120, 3191-3198, 2015.

823 Yang, K., Koike, T., and Ye, B.: Improving estimation of hourly, daily, and monthly
824 solar radiation by importing global data sets, *Agric. For. Meteorol.*, 137, 43-55,
825 2006.

826 Yang, L., Cao, Q., Yu, Y., and Liu, Y.: Comparison of daily diffuse radiation models in
827 regions of China without solar radiation measurement, *energy*, 191, 2020.

828 Yang, S., Wang, X. L., and Wild, M.: Homogenization and Trend Analysis of the 1958–
829 2016 In Situ Surface Solar Radiation Records in China, *J. Clim.*, 31, 4529-4541,
830 2018.

831 Yang, X., Zhao, C., Zhou, L., Wang, Y., and Liu, X.: Distinct impact of different types
832 of aerosols on surface solar radiation in China, *J. Geophys. Res. Atmos.*, 121, 2017.

833 Yang, Y., Ding, L., and Wang, D.: Experiments and analysis of pyranometer on
834 nighttime zero offset, *Meteorol. Mon.*, 36, 100-103, 2010.

835 Yeom, J. M., Park, S., Chae, T., Kim, J. Y., and Lee, C. S.: Spatial Assessment of Solar

836 Radiation by Machine Learning and Deep Neural Network Models Using Data
837 Provided by the COMS MI Geostationary Satellite: A Case Study in South Korea,
838 Sensors (Basel), 19, 2019.

839 Zell, E., Gasim, S., Wilcox, S., Katamoura, S., Stoffel, T., Shibli, H., Engel-Cox, J., and
840 Al Subie, M.: Assessment of solar radiation resources in Saudi Arabia, Sol. Energy,
841 119, 422-438, 2015.

842 Zhang, X., Liang, S., Wang, G., Yao, Y., Jiang, B., and Cheng, J.: Evaluation of the
843 reanalysis surface incident shortwave radiation products from NCEP, ECMWF,
844 GSFC, and JMA using satellite and surface observations, Remote Sens., 8, 225-
845 249, 2016.

846 Zhang, X., Liang, S., Wild, M., and Jiang, B.: Analysis of surface incident shortwave
847 radiation from four satellite products, Remote Sens. Environ., 165, 186-202, 2015.

848 Zhang, Y., Rossow, W. B., Lacis, A. A., Oinas, V., and Mishchenko, M. I.: Calculation
849 of radiative fluxes from the surface to top of atmosphere based on ISCCP and other
850 global data sets: Refinements of the radiative transfer model and the input data, J.
851 Geophys. Res. Atmos., 109, 2004.

852 Zhao, L., Lee, X., and Liu, S.: Correcting surface solar radiation of two data
853 assimilation systems against FLUXNET observations in North America, J.
854 Geophys. Res. Atmos., 118, 9552-9564, 2013.

855 Zhou, Q., Wang, C., and Fang, S.: Application of geographically weighted regression
856 (GWR) in the analysis of the cause of haze pollution in China, Atmospheric
857 Pollut. Res., 10, 835-846, 2019a.

858 Zhou, Z., Lin, A., Wang, L., Qin, W., zhong, Y., and He, L.: Trends in downward surface
859 shortwave radiation from multi-source data over China during 1984–2015, Int. J.
860 Climatol., 40, 1-19, 2019b.

861 Zou, L., Wang, L., Lin, A., Zhu, H., Peng, Y., and Zhao, Z.: Estimation of global solar
862 radiation using an artificial neural network based on an interpolation technique in
863 southeast China, *J. Atmos. Sol. Terr. Phys.*, 146, 110-122, 2016.

864

865